Accepted Manuscript

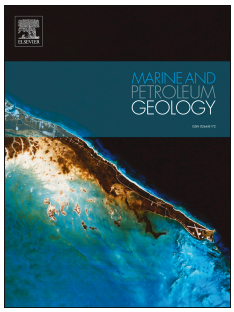

Quantification of the magnitude of net erosion in the southwest Barents Sea using sonic velocities and compaction trends in shales and sandstones

Dimitrios Ktenas, Erik Henriksen, Ivar Meisingset, Jesper Kresten Nielsen, Karin Andreassen

PII: S0264-8172(17)30369-0

DOI: 10.1016/j.marpetgeo.2017.09.019

Reference: JMPG 3077

To appear in: *Marine and Petroleum Geology*

Received Date: 20 January 2017

Revised Date: 15 September 2017

Accepted Date: 15 September 2017

Please cite this article as: Ktenas, D., Henriksen, E., Meisingset, I., Nielsen, J.K., Andreassen, K., Quantification of the magnitude of net erosion in the southwest Barents Sea using sonic velocities and compaction trends in shales and sandstones, *Marine and Petroleum Geology* (2017), doi: 10.1016/j.marpetgeo.2017.09.019.

Quantification of the magnitude of net erosion in the southwest Barents Sea using sonic velocities and compaction trends in shales and sandstones

Dimitrios Ktenas[a,b,*], Erik Henriksen[a,b], Ivar Meisingset[c], Jesper Kresten Nielsen[d] and Karin Andreassen[e]

[a] Research Centre for Arctic Petroleum Exploration (ARCEx), Department of Geosciences, University of Tromsø - The Arctic University of Norway, Dramsveien 201, NO-9037 Tromsø, Norway

[b] North E&P AS, Tjuvholmen Allé 3, NO-0252 Oslo, Norway

[c] First Geo AS, Karenslyst Allé 57, NO-0277 Oslo, Norway

[d] MOL Norge AS, Trelastgata 3, NO-0191 Oslo, Norway

[e] Centre for Arctic Gas Hydrate Environment and Climate (CAGE), Department of Geosciences, University of Tromsø - The Arctic University of Norway, Dramsveien 201, NO-9037 Tromsø, Norway

*Corresponding author. E-mail: dimitriosktenas@gmail.com

ABSTRACT

During specific intervals within Mesozoic and Cenozoic times, several areas of the southwestern Barents Sea were subjected to uplift and erosion. Areas with missing shallow stratigraphic interval sections and major erosion can be seen at several places along interpreted regional profiles in the southwestern Barents Sea. A new Normal Compaction Trend (NCT) for two selected shale– and sandstone–dominated lithologies has been constructed based on sonic logs in the southwestern Barents Sea. The shale– dominated NCT is calibrated to the Cretaceous shales in the Northern North Sea and Norwegian Sea and applied to the Cretaceous

shales of the Barents Sea. The sandstone–dominated NCT is calibrated to the Lower Jurassic Åre Formation of the Norwegian Sea and applied to the Lower Jurassic–Upper Triassic coastal plain section in the Barents Sea. By utilising the NCT model, the study estimates net apparent erosion in 28 selected Barents Sea wells based on comparison of sonic log velocities. A net apparent erosion map of the study area was constructed by gridding of the well values. The accuracy of the map is limited in areas with little well control, such as in the northwest, where the east–west transition into the southwestern Barents Sea region is poorly constrained. With that in mind, the map clearly shows two regional trends which dominate the erosion pattern in the study area; an increasing amount of erosion towards the north and a sharp decrease of erosion westwards of the hinge zone into the southwestern Barents Sea. The highest erosion estimates are observed towards Svalbard, with values up to 2500 m. The results of this study can be further utilized in petroleum system studies in the eroded areas.

Keywords: Normal Compaction Trend (NCT), net apparent erosion, maximum burial, shale compaction, southwestern Barents Sea

1. Introduction

As part of the Norwegian Continental Shelf (NCS), the southwestern Barents Sea is generally ice–free and more accessible than any other continental shelf in the Arctic. It also corresponds to one of the frontier areas that is currently open for hydrocarbon exploration.

After drilling of the first exploration wells in the Barents Sea in the early 1980s, the issue of uplift and erosion has been much debated in academia and in the oil industry.

The southwestern Barents Sea area (Fig. 1) has been subjected to several phases of uplift and erosion during Mesozoic and Cenozoic times, resulting in a profound impact on the petroleum systems (Henriksen et al., 2011a). Along the southern flank of the Barents Sea, the Finnmark Platform is a characteristic example of an area that has undergone major uplift, this can be clearly seen on the seismic sections and regional interpreted profiles (Fig. 2 and 3). There is still a debate in academia and in the petroleum industry about the magnitude and timing of the erosional products especially from the Cenozoic uplift. This is a research question of great importance for the petroleum industry with regards to play and prospect evaluation in undrilled areas.

The Norwegian explorer Fridtjof Nansen (1904) was the first to suggest that substantial uplift (of ~500 m) and deep erosion has occurred both onshore and offshore, on the Barents Shelf, during Cenozoic time. Later studies of the magnitude and timing of uplift and erosion have used many different methodologies, including compaction estimation (sonic log and refraction velocity depth trends), diagenesis of clay minerals, fluid inclusions, anomalous seismic velocities, seismic sequence geometries, volumetric mass balance studies, apatite fission track analysis, vitrinite reflectance and basin modelling (e.g. Vorren et al., 1991; Nyland et al., 1992; Riis and Fjeldskaar, 1992; Eidvin et al., 1993; Løseth et al., 1993; Richardsen et al., 1993; Reemst et al., 1994; Sættem et al., 1994; Fiedler and Faleide, 1996; Rasmussen and Fjeldskaar, 1996; Lerche, 1997; Dimakis et al., 1998; Elverhoi et al., 1998;

Butt et al., 2002; Cavanagh et al., 2006; Ohm et al., 2008; Green and Duddy, 2010; Henriksen et al., 2011a; Laberg et al., 2012; Duran et al., 2013, Baig et al., 2016, Zattin et al., 2016).

The timing of the several phases of uplift and erosion as well as the maximum burial of the sedimentary sequences represents a key factor in assessing the exploration potential of frontier areas (e.g. Green and Duddy, 2010). A series of papers (Vorren et al 1991; Riis and Fjeldskaar, 1992; Eidvin et al., 1993; Løseth et al., 1993; Mørk and Duncan, 1993; Fiedler and Faleide, 1996; Hjelstuen et al., 1996; Laberg et al., 2012) suggests a dominant phase of Late Pliocene to Pleistocene exhumation. They describe the presence of Cenozoic clastic wedges of young glaciogenic sediments along the western margin of the Barents Sea and Svalbard, related to several phases of glacial erosion followed by isostatic compensation during the last ~2.7 Ma (Rasmussen and Fjeldskaar, 1996). In addition, Andreassen et al. (2007; 2009) documented in more detail the importance of glaciotectonism for the evolution of the Barents Shelf, and that erosion rates were higher where former glacial ice streams flowed. Studies from the North Slope of Alaska (Green and Duddy, 2010), the Western Canada Basin, the Sverdrup Basin (Arne et al., 2002), Svalbard (Blythe and Kleinspehn, 1998), West Greenland (Japsen et al., 2005) and East Greenland (Thomson et al., 1999; Hansen et al., 2001) describe regions subjected to significant Cenozoic exhumation similar to the Barents Sea.

The purpose of this study is to quantify the amount and regional variation of uplift and erosion in the southwest Barents Sea using best practice industry techniques. In order to avoid confusion concerning the terminology of uplift and erosion, it was proposed by Henriksen et al. (2011a) to use the term "net apparent erosion". This is the difference between the maximum

burial depth and present–day burial depth for a specific horizon. By adding the erosion value to the present depth, information about the maximum burial depth can be obtained.

The method used for the net apparent erosion estimates is based on shale and sandstone compaction. The study uses velocity data from 40 wells located on the Norwegian Continental Shelf (NCS), 28 in the southwestern Barents Sea study area and 12 reference wells in Norwegian Sea and North Sea. The reference wells were used to construct velocity depth-trends for shale– and sandstone–dominated sedimentary sequences. The interpretation of the velocity–depth trends has led to the construction of a new Normal Compaction Trend (NCT) model for the southwestern Barents Sea. The NCT model for shale– and sandstone–dominated lithologies was further used to estimate net apparent erosion from sonic logs in available wells.

2. Study area and geological setting

The main study area is located in the southwestern Barents Sea (Fig. 1). Well log data from other parts of the NCS were analysed in order to compare the Barents Sea with areas with little or no uplift (Norwegian Sea and North Sea). The Barents Sea is an epicontinental sea with an average depth of 230 m and a maximum depth reaching 500 m (Butt et al., 2002). It developed as an intra-cratonic basin from the Late Devonian, includes of a number of basins, platforms and basement highs and is underlain by Caledonian basement rocks (Fig. 4) (Faleide et al., 1993; Smelror et al, 2009). Evidence from a pseudo–gravity field in Finnmark County shows the extension of the Caledonian front (Henriksen et al., 2001b; Gernigon et al., 2014; Nasuti et al., 2015).

Following the Caledonian orogeny, the basement topography was covered by Devonian–Carboniferous strata. Faleide et al. (1993, 2008) divided the post–Caledonian history of the western Barents Sea into three significant extensional rift phases. The crustal extension during the Late Paleozoic led to the development of half–grabens (e.g. Hammerfest Basin) in the southwestern Barents Sea (Rønnevik and Jacobsen, 1984; Faleide et al., 1993; Worsley, 2008; Henriksen et al., 2011b). The onset of collision in the Uralian Orogeny during the Devonian and Carboniferous–Permian led to the subsequent uplift to the east of the Barents Sea and acted as a main source for Triassic sediments in the western Barents Sea (Ritzmann and Faleide 2009, Henriksen et al., 2011b). To the west, major faults facilitated post–Permian subsidence and separated the Hammerfest Basin by major faults, from the Loppa High and the Finnmark Platform (Smelror et al., 2009) (Fig. 3).

Later extensional tectonics shifted westwards, with Late Jurassic rifting in the Hammerfest Basin, Cretaceous subsidence in basins along the western margin and Cenozoic subsidence due to the opening of the Norwegian-Greenland Sea during Paleocene-Eocene (Faleide et al., 1993; Tsikalas et al., 2012). The Cenozoic subsidence can be also seen in Figure 3 towards the Sørvestsnaget Basin and Vestbakken Volcanic Province (Faleide et al. 1993; Henriksen et al., 2011b). These features are both bounded by oceanic crust developed during the Early Eocene (Henriksen et al., 2011b) – Oligocene, leading to subsidence (Ryseth et al., 2003). Since then the area of the Barents Sea has been affected by repeated phases of uplift and erosion and the eroded sediments have been transported and deposited to the northern and western margins (Vorren et al, 1991; Faleide et al., 1996; Laberg et al., 2012; Baig et al., 2016).

The tectonostratigraphic evolution and paleogeographic changes since the Caledonian orogeny have been extensively described in detail by several authors (e.g. Henriksen, 2011b).

The regional profile A-A' illustrates the changes in structural style and geometries and the gross stratigraphy (Fig. 3). To the west, thick wedges of preserved Paleogene-Neogene deposits testify to the Cenozoic erosion of the Barents Sea, and are also linked to the opening of the Norwegian-Greenland Sea (e.g. Faleide et al. 1993). The Sørvestsnaget Basin, Bjørnøya Basin and other basins towards the western margin are characterized by thick Cretaceous units (Henriksen et al., 2011b).

In contrast, to the east in the Barents Sea, thick units of Paleozoic and Mesozoic strata with a dominant Base Cretaceous regional unconformity (BCU) can be mapped (Henriksen et al., 2011b). A prominent Upper Regional Unconformity (URU), representing the base of the Quaternary strata, can be mapped regionally (Fig. 3). This major unconformity is an outcome of the Paleogene uplift and erosion in the Greater Barents Sea to the east of the western margin (Riis and Fjeldskaar 1992; Riis 1996; Henriksen et al., 2011a, 2011b). The Plio-Pleistocene erosional products can be also seen along the profile A-A' as described by several authors (e.g. (Vorren et al., 1991; Richardsen et al., 1991; Ryseth et al., 2003) (Fig. 3).

3. Database

Forty (40) wells from three separate areas were analysed (Fig. 5): namely from the Northern North Sea (3 wells), from the Norwegian Sea (9 wells) and from the main study area, the southwestern Barents Sea (28 wells). It was necessary to investigate areas that have not experienced uplift and erosion in order to establish a zero erosion reference point for the new NCT model and after that to investigate the southwestern Barents Sea area, which has been subjected to significant uplift and erosion. Figure 6 shows the locations of the 28 studied wells

covering a large part of the southwestern Barents Sea. The sediments in the studied wells are mainly of Paleogene to Triassic age and have been subjected to Cenozoic uplift and erosion (e.g. Nyland et al., 1992; Friedler and Faleide, 1996; Dimakis et al., 1998; Henriksen et al., 2011a; Laberg et al., 2012; Baig et al., 2016).

Of the nine wells from offshore Mid Norway investigated in this study, two are located on the Sør High, six in the Haltenbanken area and one in the Møre Basin (Fig. 5). The Northern North Sea wells added as supporting data. The tectonostratigraphic evolution of the Haltenbanken area has been summarized by Gage and Doré, 1986, Dalland et al. (1988), Ehrenberg et al. (1992) and Blystad et al. (1995). The easternmost area of the Trøndelag Platform was subjected to Cenozoic uplift and erosion (e.g. Hansen, 1996). The Haltenbanken area has been separated into three different pressure regions. In general, the highest pressure areas are confined to the deeper western region (Karlsen et al., 2004; Storvoll et al., 2005; Van Balen and Skar, 2000; Borge, 2002; Lothe et al., 2004). The wells have penetrated sediments from Cenozoic to Mesozoic age and have been selected to represent a range of structural settings from shallow platform areas (Sør High and Horda Platform) to a deep basin (Møre Basin). The reference area wells have not been subjected to uplift because they are located geographically towards the west, far away from the Norwegian coastline.

The sonic logs from 40 exploration wells along the Norwegian shelf were imported and thoroughly quality checked (Fig. 5 and 6). The primary data sources (time-depth curve, well path, sonic logs (DT), well tops and well reports) were provided from the Norwegian Petroleum Directorate (NPD) web pages and Norwegian Diskos National Data Repository (Diskos) database. Any erroneous or low quality time-depth-velocity data were removed, in particular at the top and the bottom of each of the individual logging runs. Invalid curve data

recorded due to logging operations within borehole casing, were also removed. Deviated wells were converted to True Vertical Depth Sub Seabed (TVDSS). As shown in Table 1, there is an abbreviated list of the well tops from NPD used for the velocity vs. depth plots in the Norwegian Continental Shelf. This was needed to set up well tops as a set of common names that could be consistent for the whole NCS.

In addition to the quantitative evaluation of the net apparent erosion by studying the compaction trends of the well logs, regional seismic profiles A-A' and B-B' have been interpreted. The composite 2D lines were constructed from different 2D seismic surveys that are partly public from NPD Diskos database. Well log data from wells located in the vicinity of the 2D seismic lines were also integrated (Fig. 2 and 3, for the location of the profiles and tied–to–seismic wells see Fig. 1). In the wells, information on formation tops for a well–to–seismic tie was important for the seismic interpretation in order to identify and delineate the stratigraphy. This also helped to gain understanding of the lithological variation, fluid content and geophysical characteristics of the subsurface.

4. Method

4.1 Establishment of a new NCT model

Defining normal compaction trends using sonic velocity vs. depth base lines, is an established exploration geophysical method, and several mathematical formulations have been introduced to describe the increase of velocity with depth, in a manner similar to porosity (e.g. Wyllie et al., 1956; 1958; Athy, 1930). Many authors have published exponential equations or other linear trends to define compaction trends for shale or other lithologies (Hottmann and

Jonson, 1965; Magara 1976; Scherbaum, 1982; Sclater and Christie, 1980; Baldwin and Butler, 1985; Bulat and Stoker, 1987; Wells, 1990; Issler, 1992; Hillis, 1995; Japsen, 1993, Hansen, 1996; Heasler and Kharitonova, 1996; Japsen, 2000; Storvoll et al., 2005; Japsen et al., 2007; Mondol, 2009; Tassone et al., 2014; Baig et al., 2016).

Two sets of NCT curves which have been tested extensively with many rock types in basins worldwide are from Japsen et al. (2000, 2007) and First Geo (unpublished, based on Gardner et al., 1974). They are based on different data, and as shown in Figure 7 they look quite different. Whereas Gardner et al. (1974) based his curves on clean sands and shales picked from well logs in young sedimentary basins (Gulf of Mexico area), Japsen et al., (2000; 2007) used interval velocities from consolidated Jurassic and Triassic shale- and sandstone-dominated formations from wells in the UK and Danish North Sea Basin. Figure 8 shows the Japsen and First Geo NCT models plotted together with reference wells 31/4-3 from the Northern North Sea well and 6305/1-1 T2 from the Norwegian Sea. The former is from a shallow platform with thick Triassic, the latter from a deep basin (Møre Basin) with an ultra-thick Cretaceous sequence. The First Geo "Gardner" shale baseline gives a reasonable fit to well 6305/1-1 T2, except for the (Tertiary) diatomite sections where the velocities are extremely low. The "Japsen" sand line gives a reasonable fit to the Jurassic-Triassic section in well 31/4-3. This demonstrates the difficulty of making one NCT model which fits all wells and lithologies and illustrates the need to develop a new, independent NCT model for use in the southwestern Barents Sea.

The velocity depth-trend or baseline (Japsen et al., 2007), (synonym of NCT used in this study) describe how the velocity increases with depth in a formation, with relative

homogeneous brine saturated sedimentary formation when the porosity is reduced during normal compaction (mechanical or chemical). The NCT model referred to in this study corresponds to a set of curves, whereby a NCT is a curve or a straight line that is used as a trend line against a log curve (two in this study). Comparison between the NCT model and the actual compaction trend also allows identification of zones of overcompaction and undercompaction (e.g. Heasler and Kharitonova 1996; Japsen et al., 2000). The existence of such zones will also give information on the amount of removed overburden (e.g. Bulat and Stoker, 1987; Corcoran and Doré 2005), on estimating overpressure due to undercompaction (e.g. Japsen 1998; 1999; 2000), on depth conversion of seismic data (Al-Chalabi, 1997), on stratigraphic velocity interpretation (Peikert, 1985) and on amplitude variations with offset (AVO) on seismic data (e.g. Smith and Sondergeld, 2001).

A new NCT model has been developed for the southwestern Barents Sea. Well logs from this study have been used to establish the calibration curves which describe the NCT model for a given rock type as a function of depth. The workflow for establishing a new NCT model and a net apparent erosion map is shown in Fig. 9. All the information from the wells in the southwestern Barents Sea was gathered and reference wells from the North Sea and Norwegian Sea with zero net erosion were carefully studied. As a first approach, based on a review of published and unpublished baselines, these were applied to the reference wells. While matching the baselines against the well logs in the Norwegian Sea, the same baselines using deep wells for the Paleogene and Cretaceous shale layers were applied to the southwestern Barents Sea. Then, after the adjustment of the baselines, these baselines were extended deeper, down to the Lower Jurassic and Triassic sections in the southwestern Barents Sea. When a good match between the baselines for shale and sandstone had been obtained, a

new NCT model was constructed (Fig. 10). In this study, these two baselines will be called "Dikte NCT model" calibrated for the Cretaceous shale (CretShale) and Lower Jurassic–Triassic (LJurTrias) sequences which correspond to mixed sand-shale lithologies. The baselines in the combined set work together, and represent the normal compaction of a multi-lithology system.

4.2 Interpretation of the net apparent erosion

In general, a porous rock will compact as a result of the effective stress and will therefore have an appropriate normal compaction trend line. A deviation from normal compaction, for a given lithology, can be interpreted as a measurement of net apparent erosion (Fig. 11). The result of the process of aligning the wells with the zero net erosion baselines has the effect of adjusting the depth of the wells to maximum depth of burial while keeping the baseline fixed.

After establishing a NCT model based on well log data, three main stages were followed to establish a net apparent erosion map:

1) A stratigraphic layer was selected as a basis for the analysis (shale or other lithologies).

2) Net apparent erosion was estimated in the wells, following the method shown in Figure 11.

3) The well estimates were gridded and contoured. Conflicting values in neighbouring wells were investigated and reinterpreted to achieve a consistent and geologically reasonable pattern of uplift and erosion.

4.3 Geological constraints on the net erosion estimates

There are two fundamental geological constraints on the shale compaction method. The first is that the reference wells must have zero net apparent erosion. The second is that the net apparent erosion must be estimated from the compaction of the same type of rock in the reference and study areas.

In this study, the reference wells in the Northern North Sea and in the Norwegian Sea did not have zero net apparent erosion. There was a small amount of glacial erosion of the seabed, with bearing seabed topography and one well that was affected by the Storegga slide. We decided to estimate the amount of these erosions and to compensate for them. In the Norwegian Sea and in the Northern North Sea areas we assumed that a pre-glacial erosion seabed had existed as a flat surface 100 m below present-day sea level. This suggested value is compatible to what has been published by several workers (e.g. Sejrup et al., 2003), assuming that the terrain west of the Norwegian trench was formed by the effects of the glacial fluvial erosion processes during the late Cenozoic. In the Storegga slide area we used a reconstructed slide seabed (First Geo, unpublished). The difference in each well, between the present-day water depth and this estimated pre-glacial water depth was added as a net apparent erosion correction. This had the effect of eliminating the topographic variation in water depth from well-to-well due to the eroded seabed landscape. There is some uncertainty related to the 100 m pre-glacial water depth assumption, but this is small compared to the general uncertainty of the southwestern Barents Sea net apparent erosion estimates.

The Cretaceous shales in the Norwegian Sea and the southwestern Barents Sea are thought to be of the same litho-facies type and to be very suitable for net apparent erosion estimates. On closer inspection, we found that these shales in the Norwegian Sea, and the Northern North Sea display a small amount of compaction disequilibrium. This is evident from comparison of the Upper Cretaceous thick massive claystones in well 6305/1-1 T2, (Fig. 8) with the shale baselines of "Japsen" and First Geo "Gardner" NCT models. These NCT models have been widely used, and the general relationship between shale baselines and compaction disequilibrium is well known (First Geo; Japsen P., pers. com.). A degree of compaction disequilibrium, and perhaps a moderate disequilibrium overpressure, is typical for massive shale units in active sedimentary basins worldwide. In our assumption, that the Norwegian Sea wells are good reference wells for the southwestern Barents Sea, there in an implicit assumption that the state of compaction disequilibrium in the southwest Barents Sea wells, at the onset of the uplift and erosion, was identical to the state of disequilibrium compaction in the Norwegian Sea wells at the present day. There is no way to know if this was actually the case, however we considered these assumptions to be reasonable since the geological history of these areas at these times was reasonable similar. The compaction disequilibrium in the Norwegian Sea today is moderate. If it was not similar to the Barents Sea during the onset of the uplift, then it is more likely to have been larger than smaller especially in the western most part of the Barents Sea where the shale units are thicker. A larger compaction disequilibrium means lower compaction relative to depth of burial and lower velocity. The shale compaction method will therefore underestimate the net apparent erosion in wells where this has occurred.

The sand-dominated Triassic sections which exist in thick deposits in the Barents Sea, Norwegian Sea and Northern North Sea areas have similar proportions of clay and sand, but

the compaction behaviour is very different. When we plotted the data we found them to group together on the basis of their depositional environment. The Lower Jurassic-Upper Triassic of the southwest Barents Sea was deposited in a coastal plain environment with some marine influence. A typical formation is the Fruholmen Formation (Norian to Rhaetian age). A typical formation of the Norwegian Sea area is the Åre Formation (Rhaetian-Pliensbachian). This is also a coastal to plain deposit. These coastal plain deposits from the Norwegian Sea and the Barents Sea seems to follow the same velocity vs. depth relationship and the same NCT baseline. The Triassic sections of the Norwegian Sea and the Northern North Sea were deposited in a desert environment and are shown with higher velocity with respect to the depth of burial. These were investigated as possible references for the Triassic for the southwest Barents Sea but had to be rejected. It seems that "sand" or "sand dominated" are not sufficient criteria for grouping lithologies for uplift and erosion studies. It is also necessary to have similar depositional environments.

5. Results and Discussion

5.1 Net apparent erosion estimates from reference areas

Figure 12 shows the primary reference wells from the Norwegian Sea and one well from the Northern North Sea that have been calibrated to zero erosion for specific stratigraphic units; the shale-dominated Cretaceous lithologies and the sandstone-dominated Lower Jurassic. The correction value for the glacial/Storegga Slide erosion is given in the upper right corner of each well plot. Figure 12 shows the NCT base lines from Figure 10 plotted together with sonic

velocity against maximum depth of burial. The objective of the reference well study was to obtain a best possible fit of zero erosion NCT base lines against the selected lithologies.

The primary NCT base line from the Norwegian Sea wells is the shale base line. This aligns very well with thick Cretaceous shale sections in all three Norwegian Sea wells in Figure 12. In well 6406/6-1, the alignment is very good from near Top Cretaceous (TC) through Top Cromer Knoll (Cromer). The uppermost Cretaceous has a lower velocity than the base line, grading upwards into the Lower Tertiary where there is a velocity inversion. This inversion is typical for the Norwegian Sea as well as for the North Sea, and it makes the Tertiary section difficult to use as a reference section for erosion studies. The upper part of the Tertiary, which lies on the sandstone base line, is the prograding, glacially derived Pleistocene section. In well 6506/12-1 the log pattern is very similar, but the velocity variation in the Upper Cretaceous is slightly more variable and the fit to the base line is not quite as good. Both of these wells have mixed sand-shale lithologies in the Upper Cretaceous, but the dominating lithology is shale. Well 6305/1-1 T2 from the Møre Basin has a much thicker Cretaceous section with "cleaner shales". The BC horizon plotted at the base of the log is at Total Depth (TD), indicating that the age of the unit above TD is Cretaceous. This well shows a very good match with the shale base line and shows that the same base line works for wells with medium and very large stratigraphic thickness in the Cretaceous. Well 30/2-1 from the Northern North Sea does not give a good match. There is a partial match to a shale unit within the Upper Cretaceous and the lowermost Tertiary Lista Formation. The Uppermost part of the Cretaceous (Maastrichtian) in this well has some sandstone and siltstone, which is a distal equivalent to the Maastrictian limestones which developed further south and southeast in the Northern North Sea. This is indicated by a velocity increase as seen in Figure 12. This well matches the shale

baseline in the Lower Jurassic Drake Formation. This is different from how the Jurassic shales behave in the Norwegian Sea area.

It was required for the sandstone NCT baseline to support the same net apparent erosion estimate in the southwestern Barents Sea wells as it was done by the shale NCT base line. Therefore, the determination of the sandstone NCT baseline was based on both, the southwestern Barents Sea wells as well as the Norwegian Sea wells. It was found that the Lower Jurassic–Upper Triassic section in the Barents Sea followed the same NCT baseline for the Lower Jurassic section in the Norwegian Sea area, and in particular the Åre Formation.

Well 6506/12-1 is the primary reference well for the Lower Jurassic sandstone NCT base line in the Norwegian Sea area. It has a thick Åre Formation from about 4300 m to 4800 m maximum burial depth at the base of the well, to which the sandstone NCT base line gives a very good match. A very good match between the sandstone NCT baseline and the Åre Formation has also been identified in well 6608/10-2 from about 2700 m to 3500 m and in well 6507/6-4A from about 900 m to 1100 m maximum burial depth. Well 7120/9-2 was our key well for calibration of the sandstone NCT baseline in the southwestern Barents Sea (Fig. 13). This well has a thick Lower Jurassic–Upper Triassic section from about 3500 m to 5000 m of maximum depth of burial.

5.2 Net apparent erosion estimates in the southwestern Barents Sea

Figure 13 shows the new Dikte NCT model developed for the southwestern Barents Sea applied to the sonic logs against the maximum burial depth. The interpretation on the net

apparent erosion estimates is based on the Cretaceous shales and Lower Jurassic-Upper Triassic sections and the values are given in the upper right corner in Figure 13. The primary NCT baseline for the determination of the net apparent erosion in the southwestern Barents Sea wells was the shale NCT baseline. The shale NCT baseline was established with great confidence from the closest reference area wells in the Norwegian Sea as well as in the Northern North Sea. Therefore, many wells in the southwestern Barents Sea could be determined from the shale NCT baseline (e.g. well 7121/5-3, Fig. 13).

Among the 28 wells studied in the southwestern Barents Sea, the wells 7129/9-2, 7121/5-1 and 7121/5-3 were some of the good representatives using the shale NCT baseline for estimating the net apparent erosion for the southwestern Barents Sea (Fig. 13). The same wells were also helpful to define the alignment position of the sandstone NCT baseline. Well 7321/7-1 has a thinner stratigraphic section of Cretaceous shales compared to the other wells. The lithofacies development in the Cretaceous section is showing a poor match with the shale NCT baseline. In this well the net erosion estimate is mainly based on the sandstone NCT baseline. However, the Dikte NCT model has always been considered to work as a consistent set of baselines working together and the wells were inspected to look for good alignment either for thick or thin lithofacies.

There is no other Triassic section in the NCS which is quite similar to the southwestern Barents Sea. Hence, it was not easy to determine a sandstone baseline in the southwestern Barents Sea. However, we were more confident about the determined shale baseline in the Norwegian Sea where there is geological similarity to the southwestern Barents Sea Cretaceous shales. When we interpret the amount of net apparent erosion in each of the Barents Sea wells the first step is to use the established shale NCT baseline where the thick Cretaceous shales are present. It is well known that the Triassic section in the southwestern

Barents Sea is more extensive compared to the Cretaceous section at the same area (e.g. see Profile A-A', Fig. 3). Thus, the next step was to investigate many other wells whereas the net apparent erosion values were measured from Triassic sections against the sandstone NCT baseline (e.g. 7324/10-1, 7229/11-1, 7222/11-1 T2 and 7321/7-1, Table 3).

The sandstone NCT baseline gives a good match with the Lower Jurassic-Upper Triassic sections in all the four wells as shown in Figure 13. In well 7120/9-2 there is a good alignment with the sandstone NCT baseline from Base Cretaceous (BC) through (InBTr). In well 7121/5-1 the sandstone NCT baseline shows a good match with the sonic velocity from 3600 m to 4500 m maximum burial depth. Similar quality of the match is shown in well 7121/5-3 from Lower Jurassic through to Intra Base Triassic (InBTr). Furthermore, the well 7321/7-1 shows a good fit with the sandstone NCT baseline from the Lower Jurassic to the Lower Triassic. From the overall alignment of the well logs studied in the southwestern Barents Sea it was concluded that the sandstone NCT baseline is efficient for silty-sandy lithologies.

During the interpretation of the net apparent erosion some of the studied wells proved to be problematic. For example, in the westernmost area in the Barents Sea the wells 7316/5-1 and 7216/11-1S were more complicated. There are both not deep wells and the Tertiary section could not give a good match against the Dikte NCT model. Therefore, for the well 7216/11-1S the net erosion estimate provided in Table 3 corresponds to the present water depth which is 361 m. This estimate is also based on the assumption of previous works (e.g. Butt et al., 2002), that the water depth in the southwestern Barents Sea prior to the onset of glaciations was ~0 m below the present sea level.

Figure 14 shows the sonic velocity measurements vs. maximum depth of burial for the deep exploration wells 7128/6-1 and 7128/4-1 on the Finnmark Platform. In well 7128/6-1 a

relative good match between the sandstone NCT with the sonic log has been identified from 2300 m to 2800 m of maximum depth of burial. The net erosion estimate has been picked from the Lower part of the Triassic section. The InBTr is a horizon that represents the base of the Triassic section that matches the sandstone NCT baseline. Similar alignment with the sandstone NCT has been identified in well 7128/4-1 from 1800 m to 2300 m of maximum depth of burial. It is typical in the structural high of the Barents Sea that the top of the Triassic is close to the seabed which has been eroded later/or recently. Our study supports the idea that the Triassic section in these areas is related to the maximum depth of burial prior to the latest erosion as we cannot see differences in the net apparent erosion between the Late Jurassic horsts and grabens. Several studies have shown that carbonates can also be used for uplift and erosion estimates (e.g. Schmoker and Halley, 1982).

The amount of net apparent erosion decreases towards the continental margin and is outlined at around ~300 m in the western part of the Barents Sea. The highest erosion values are observed towards Svalbard with values reaching ~2500 m. The present seabed topography (Fig. 6) seems to reflect the degree of erosion. The areas on the platform with least water depth correspond approximately to areas with the highest net apparent erosion (Fig. 15). Two different trends of net apparent erosion are observed; an increase along a south to north direction and a decrease from southeast to northwest. In the northwestern part of the study area, the rate of change of net erosion is much faster due to the close spacing of the isopachs. Due to the lack of well data, there is uncertainty in the net apparent erosion values in areas with total absence of well information, (e.g. in the northeastern part of the Barents Sea study area).

The erosion map from Nyland et al. (1992) (Fig. 16) showed that about 1200 m of uplift and corresponding erosion had occurred in the southwestern Barents Sea, while a

thickness of about 3100 m of sediment had been removed from the Svalbard drainage area. Their studies were based on a map of the Upper Regional Unconformity (URU) (see also Fig. 3), combined with bathymetric maps and a drainage system map of the Barents Shelf, together with volumetric calculations of the western fans. Doré and Jensen (1996) calculated that 0–500 m of overburden have been removed from the Hammerfest Basin, Senja Ridge and Tromsø Basin, 100–1500 m from the remaining Hammerfest Basin and Loppa High, 1500–2000 m from the Finnmark Platform and over 2000–3000 m from the Stappen High area. For the southwestern Barents Sea sedimentary basins, Henriksen et al. (2011a) suggested net erosion magnitudes between 900 and 1400 m and further to the west minor or zero net erosion. In the Hammerfest Basin and Nordkapp Basin, the erosion reached magnitudes between 1000–1400 m and for the northernmost well in the Bjarmeland Platform ~1700 m. Baig et al. (2016) based on different methods (three data sources), including sonic well logs, constructed a net exhumation map and suggested an average of ~0–2400 m of uplift and erosion. The same authors suggested net erosion estimates that range from ~800 to 1400 m in the Hammerfest Basin, ~1150–1590 m on the Loppa High, ~1200–1400 m on the Finnmark Platform and ~1250–2400 m on the Bjarmeland Platform.

Several net apparent erosion estimates from previous studies are summarized in Fig. 16. They all suggest a general trend of increase of uplift and net erosion towards the East and Northeast and less uplift across the basins. When comparing Figures 15 and 16, we notice that the overall mapped trends appear to be the same, but also that there are quantitative differences, plus an apparent lack of differentiation in the northern Barents Sea between the Stappen High and areas farther east. However, due to the lack of well data points in that direction, uncertainties on the parabolic gridding have been also seen (Fig. 15). In some areas discrepancies up to ~200–600 m are observed due to uncertainties and differences in how the methods are estimating net erosion (Fig. 16), based on the availability of input data.

Net apparent erosion "alignment uncertainty" estimates for each of the wells are listed in Table 3. The average uncertainty is 126 m, with a maximum of 300 m. This uncertainty is related to the similarity of the lithologies between the reference area wells and the wells in the study area. In particular, uncertainties related to vertical and lateral facies variations in the Cretaceous shales and the degree of disequilibrium prior to the uplift and erosion. The shale compaction method depends on the assumption that the state of compaction has not been changed since the uplift and erosion had started. Furthermore, the velocity was not altered since that time. The same assumption applies to the Triassic sandstones as it will create a bias on the uplift estimates. Thus, the net erosion uncertainties have been minimized using the best possible reference wells from the closest areas (Norwegian and North Sea) where no uplift and a similar geology are present. Another uncertainty in the net erosion estimates could be related to measurement errors such as the quality of the well log data and the accuracy of the sonic log as a measurement of the velocity. Another source of uncertainty lies in the choice of zero uplift reference wells and (the slope of the) base lines. This would come as a change of the absolute values and will not change the shape of the net apparent erosion map.

By combining the net erosion estimates with sub-crop and truncational events interpreted in the regional seismic profiles A-A’ and B-B’, accuracy was optimized and the areal extent of net apparent erosion map was better constrained. The main reflectors that have been interpreted in Figure 2, were identified from well log data ranging from the seabed to the Permian. Major sub-vertical faults cutting through the Mesozoic stratigraphy define the main tectonic activity. At between 270 and 400 ms, an erosional surface is observed and is interpreted as the Upper Regional Unconformity (URU, Fig. 2). The Cenozoic strata below the URU prograde towards the south-southeast. On the southeast of the Finnmark Platform an uplifted area of Cenozoic strata is observed. The lowest level affected by the uplift is approximately at 260 ms. The erosional surface can also be identified from the erosional

contact that exists between Cenozoic strata and Mesozoic-Paleozoic strata. Mesozoic and Paleozoic strata were deposited on basement and thus develop a steep inclination towards the center of the Finnmark Platform (eastern part of B-B' cross section, Fig. 2).

On the regional profile A-A' (Fig. 3) the interpreted reflectors range from the seabed to the Basement. To the east, the URU is observed at 150 ms whereas along the western margin the unconformity can be observed at depths ~700 ms. On the Loppa High missing sections of a Paleogene to Carboniferous strata can be observed. The sedimentary successions on the eastern side of the Loppa High becomes thinner away from this geological structure towards the east. The fault zone variation between the Finnmark Platform and the Sørvestsnaget Basin indicates basin extension and larger accommodation space being created for deposited sediments in the Sørvestsnaget Basin. On the flanks of the Loppa High the thickening of the sedimentary succession suggests basin opening/extension and more accommodation space for deposition (Fig. 3).

6. Conclusions

Net apparent erosion has been estimated in 28 wells in the southwestern Barents Sea (Table 3) and a computer contoured map (Fig. 15) shows two main regional trends of erosional pattern; an increasing amount of erosion towards the north and a sharp decrease of erosion westwards of the hinge zone into the western Barents Sea.

A clear empirical relationship between compaction, as measured by velocity, and the maximum depth of burial of the rocks can be obtained. From theory and empirical observation, rocks are known to become more compact as a consequence of burial and effective vertical stress. The state of compaction of an uplifted and eroded rock sequence can therefore be used

to indicate the amount of erosion. Sonic velocity values from the studied wells show that general velocity-depth trends develop as a function of shale and sand compaction processes, lithology, burial depth history and compaction disequilibrium.

It is still not known whether there was compaction disequilibrium in the Barents Sea during the onset of the uplift and erosion. In this study, it is suggested, for the first time, that the Cretaceous shales were in a situation of a compaction disequilibrium, similar to that seen in the Haltenbanken area, Norwegian Sea. Our aim was to study the compaction and acquire information about the maximum burial depth. However, the amount of the compaction disequilibrium is uncertain and the results must be regarded in this light.

In this study, the calculated net erosion estimates are based from an assumption that the NCS was flat prior to the Quaternary glacial erosions that created the present day seabed relief. In the references area, a 100 m pre-glacial water depth is assumed, which means that the flat area was 100 m deeper than the present day. In the southwestern Barents Sea, it is assumed that this had been at 0 m. These different values of the pre-glacial water depth could change, but these values were not the primary goal of this study. The degree of uncertainty is not significant and adjustments to pre-glacial water depth are only likely to comprise a few tens of meters.

Based on the available well log data, a new NCT model for the southwestern Barents Sea was developed and a net apparent erosion map was constructed. In this new "Dikte NCT model" (Fig. 10, Table 2), the calibrated baselines for the southwestern Barents Sea match the Cretaceous shales in the reference wells and also the Lower Jurassic-Triassic units which represent mixed sand-shale lithology deposited in a coastal plain to shallow marine environment. The new "Dikte NCT model" corresponds to a better representative for the

younger shale stratigraphic intervals and can address greater depths (e.g. within the Triassic) compared with other published compactions trends.

In the calibration step, comparing the baselines in the southwestern Barents Sea and the reference areas, it was concluded that it is not correct only to determine a baseline based on the age of sand-dominated rock. The depositional environment must also be considered. Similar baselines can be obtained where we have similar lithofacies and depositional environments. The new baselines match for strata from coastal environments and not (for example) "desert" environments typical of the North Sea. This study also reveals that general baselines for shale, sandstone and other lithologies (e.g. carbonates, see Fig. 14) can be generated using velocity data from well logs following the suggested work flow for establishing a NCT model (Fig. 9).

Taking into account uncertainties related with the well data and the NCT model assumptions, the quality of this work with compaction is solid and the shape of the map is reliable. The work process is mainly based on an interaction of single estimates and map displays, where at the end a regionally consistent multi-well interpretation of net apparent map is calculated. The absolute values of the net erosion estimates are critically dependent on the calibration to the reference wells and the gradient of the NCTs. Different net erosion estimates from other studies illustrate the uncertainties between different methods (Fig. 16).

The well log based NCT model can be calibrated to other velocity data such as interval velocities in maps and seismic profiles from regional depth conversion. This can be used to estimate net erosion in undrilled areas. This can be done to support the mapping of net erosion from our well study, or to continue the mapping of net erosion into areas that have not yet been drilled. This also reveals that this NCT model that was constrained can be used for accurate velocity analysis such as seismic inversion and depth conversion of seismic data, pore pressure prediction, or basin and petroleum systems modelling. Basin modelling could be undertaken

along the seismic profiles based on the observed maturity, vitrinite reflectance and present-day temperature measurements, taking into account the variability of the heat flow, which has been changed through time and the maximum burial depth.

Acknowledgements

The research received funding from the People Programme (Marie Curie Actions) of the European Union's Seventh Framework Programme FP7/2007-2013/ under REA grant agreement No 317217. The research forms part of the GLANAM (GLAciated North Atlantic Margins), www.glanam.org Initial Training Network. This is also a contribution to the RCN funded project "Research Centre for Arctic Petroleum Exploration" (ARCEx) (grant 228107). We are thankful to First Geo AS for the use of the AKGT software (First Geo's internal Geocap software) and in this context we thank Olav Egeland. Thanks to Searcher Seismic, Spectrum and TGS NOPEC ASA for being allowed to publish the seismic data. Many thanks to colleagues at North Energy ASA (North E&P AS) for their comments based on their work experience in the Barents Sea. Anthony M. Spencer and Tony Doré are both acknowledged for their constructive comments. Further, we greatly appreciate the two anonymous reviewers for their contribution improving the manuscript.

Appendix A. Supplementary data

Supplementary data related to this article can be found at: [a weblink referring to an attached Excel file for Table 2].

References

Al□Chalabi, M., 1997. Time□depth relationships for multilayer depth conversion. Geophys. Prospecting 45(4), 715–720.

Andreassen, K., Winsborrow, M., 2009. Signature of ice streaming in Bjørnøyrenna, Polar North Atlantic, through the Pleistocene and implications for ice-stream dynamics. Ann. Glaciol. 50, 17–26.

Andreassen, K., Odegaard, C.M., Rafaelsen, B., 2007. Imprints of former ice streams, imaged and interpreted using industry three-dimensional seismic data from the south-western Barents Sea. In: Davies, R.J., Posamentier, H.W., Wood, L.J., Cartwright, J.A. (Eds.). Seismic Geomorphology: Applications to Hydrocarbon Exploration and Production. Geological Society, London, Special Publications 277, pp. 151–169.

Arne, D.C., Grist, A.M., Zentilli, M., Collins, M., Embry, A., Gentzis, T., 2002. Cooling of the Sverdrup Basin during Tertiary basin inversion: implications for hydrocarbon exploration. Basin Res. 14, 183–205.

Athy, L. F., 1930. Density, porosity, and compaction of sedimentary rocks. AAPG Bull. 14, 1–24.

Baig, I., Faleide, J.I., Jahren, J., Mondol, N.H., 2016. Cenozoic exhumation on the southwestern Barents Shelf: Estimates and uncertainties constrained from compaction and thermal maturity analyses. Mar. Petrol. Geol. 73, 105–130.

Baldwin, B., Butler, C.O., 1985. Compaction curves. AAPG Bull. 69 (4), 622–626.

Balen, R. T., Skar, T., 2000. The influence of faults and intraplate stresses on the overpressure evolution of the Halten Terrace, mid-Norwegian margin. Tectonophysics, 320 (3), 331–345.

Borge, H., 2002. Modelling generation and dissipation of overpressure in sedimentary basins: an example from the Halten Terrace, offshore Norway. Mar. Petrol. Geol. 19 (3), 377–388.

Blystad, P., Brekke, H., Faerseth, R.B., Larsen, B.T., Skogseid, J., Tørudbakken, B., 1995. Structural Elements of the Norwegian Continental Shelf: Part II. The Norwegian Sea Region: Norwegian Petroleum Directorate Bulletin, v.8, p. 45.

Blythe, A.E., Kleinspehn, K.L., 1998. Tectonically versus climatically driven Cenozoic exhumation of the Eurasian plate margin, Svalbard: Fission track analyses. Tectonics 17, 621–639.

Bulat, J., Stoker, S.J., 1987. Uplift Determination from Interval Velocity Studies, UK Southern North Sea. In: Brooks, J., Glennie. K.W. (Eds.), Petroleum Geology of North-west Europe. Graham and Trotman, London, pp. 293–305.

Butt, F.A., Drange, H., Elverhøi, A., Otterå, O.H., Solheim, A., 2002. Modelling Late Cenozoic isostatic elevation changes in the Barents Sea and their implications for oceanic and climatic regimes: preliminary results. Quat. Sci. Rev. 21, 1643–1660.

Cavanagh A.J., di Primio R., Scheck-Wenderoth M., Horsfield B., 2006. Severity and timing of Cenozoic exhumation in the southwestern Barents Sea. J. Geol. Soc. 163, 761–774.

Corcoran, D.V., Doré, A.G., 2005. A review of techniques for the estimation of magnitude and timing of exhumation in offshore basins. Earth-Sci. Rev. 72, 129–168.

Dalland, A., Worsley, D., Ofstad, K., 1988. A lithostratigraphic Scheme for the Mesozoic and Cenozoic and Succession Offshore Mid-and Northern Norway. Oljedirektoratet.

Dimakis, P., Braathen, B.I., Faleide, J.I., Elverhøi, A., Gudlaugsson, S.T., 1998. Cenozoic erosion and the preglacial uplift of the Svalbard–Barents Sea region. Tectonophysics 300, 311–327.

Doré, A.G., Jensen, L.N., 1996. The impact of late Cenozoic uplift and erosion on hydrocarbon exploration: offshore Norway and some other uplifted basins. Glob. Planet. Change 12, 415–436.

Duran, E. R., di Primio, R., Anka, Z., Stoddart, D., Horsfield, B., 2013. 3D-basin modelling of the Hammerfest Basin (southwestern Barents Sea): a quantitative assessment of petroleum generation, migration and leakage. Mar. Petrol. Geol. 45, 281–303.

Ehrenberg, S.N., Gjerstad, H.M., Hadlerjacobsen, F., 1992. Smørbukk Field - a Gas Condensate Fault Trap in the Haltenbanken Province, Offshore Mid-Norway. AAPG Memoir 54, 323–348.

Eidvin, T., Jansen, E., Riis, F., 1993. Chronology of Tertiary fan deposits off the western Barents Sea: implications for the uplift and erosion history of the Barents Shelf. Mar. Geol. 112, 109–131.

Elverhøi, A., Hooke, R.L., Solheim, A., 1998. Late Cenozoic erosion and sediment yield from the Svalbard Barents Sea region: implications for understanding erosion of glacierized basins. Quat. Sci. Rev. 17, 209–24.

Faleide, J.I., Solheim, A., Fiedler, A., Hjelstuen, B.O., Andersen, E.S., Vanneste, K., 1996. Late Cenozoic evolution of the western Barents Sea-Svalbard continental margin. Glob. Planet. Change 12, 53–74.

Faleide, J.I., Tsikalas, F., Breivik, A.J., Mjelde, R., Ritzmann, O., Engen, O., Wilson, J., Eldholm, O., 2008. Structure and evolution of the continental margin off Norway and Barents Sea. Episodes 31, 82–91.

Faleide, J.I., Vågnes, E., Gudlaugsson, S.T., 1993. Late Mesozoic-Cenozoic evolution of the south-western Barents Sea in a regional rift-shear tectonic setting. Mar. Petrol. Geol. 10, 186–214.

Fiedler, A. Faleide, J.I., 1996. Cenozoic sedimentation along the southwestern Barents Sea margin in relation to uplift and erosion of the shelf. Glob. Planet. Change 12, 75–93.

Gabrielsen, R. H., Grunnaleite, I., Rasmussen, E., 1997. Cretaceous and Tertiary inversion in the Bjørnøyrenna Fault Complex, south-western Barents Sea. Mar. Petrol. Geol. 14, 165–178.

Gardner, G.H.F., Gardner, L.W., Gregory, A.R., 1974. Formation Velocity and Density - Diagnostic Basics for Stratigraphic Traps. Geophysics 39, 770–780.

Gage, M.S., Doré, A.G., 1986. A regional geological perspective of the Norwegian offshore exploration provinces. In: Spencer, A.M. et al. (Eds.), Habitat of hydrocarbons on the Norwegian continental shelf, pp. 21–38.

Gernigon, L., Brönner, M., Roberts, D., Olesen, O., Nasuti, A., Yamasaki, T., 2014. Crustal and basin evolution of the southwestern Barents Sea: from Caledonian orogeny to continental breakup. Tectonics 33(4), 347–373.

Green, P.F., Duddy, I.R. 2010. Synchronous Exhumation Events Around the Arctic Including Examples from Barents Sea and Alaska North Slope. In: Vining, B.A., Pickering, S.C. (Eds.), Petroleum Geology: From Mature Basins to New Frontiers – Proceedings of the 7th Petroleum Geology Conference, London. Geological Society, London, pp. 633–644.

Hansen, S., 1996. Quantification of net uplift and erosion on the Norwegian Shelf south of 66° N from sonic transit times of shale. Nor. Geol. Tidsskr. 76, 245–252.

Hansen, K., Bergman, S.C., Henk, B., 2001. The Jameson Land basin (East Greenland): a fission track study of the tectonic and thermal evolution in the Cenozoic North Atlantic spreading regime. Tectonophysics 331, 307–339.

Heasler, H.P., Kharitonova, N.A., 1996. Analysis of sonic well logs applied to erosion estimates in the Bighorn Basin, Wyoming. AAPG Bull. 80, 630–646.

Henriksen, E., Bjørnseth, H.M., Hals, T.K., Heide, T., Kiryukhina, T., Klovjan, O.S., Larssen, G.B., Ryseth, A.E., Rønning, K., Sollid, K., Stoupakova, A., 2011a. Uplift and erosion of the greater Barents Sea: impact on prospectivity and petroleum systems. In: Spencer, A.M., Embry, A.F., Gautier, D.L., Stoupakova, A.V., Sørensen, K. (Eds.). Arctic Petroleum Geology. Geol. Soc. Memoir 35, London, pp. 271–281.

Henriksen, E., Ryseth, A.E., Larssen, G.B., Heide, T., Rønning, K., Sollid, K., Stoupakova, A.V., 2011b. Tectonostratigraphy of the greater Barents Sea: implications for petroleum systems. In: Spencer, A.M., Embry, A.F., Gautier, D.L., Stoupakova, A.V., Sørensen, K. (Eds.). Arctic Petroleum Geology. Geol. Soc. Lond. Memoir 35, London, pp. 163–195.

Hillis, R.R., 1995. Quantification of Tertiary exhumation in the United Kingdom southern North Sea using sonic velocity data. AAPG Bull. Am. Assoc. Petrol. Geol. 79, 130–152.

Hjelstuen, B.O., Elverhøi, A., Faleide, J.I., 1996. Cenozoic erosion and sediment yield in the drainage area of the Storfjorden Fan. Glob. Planet. Change 12, 95–117.

Hottmann, C.E., Johnson, R.K., 1965. Estimation of Formation Pressures from Log-Derived Shale Properties. J. Petrol. Technol. 17, 717–725.

Issler, D.R., 1992. A new approach to shale compaction and stratigraphic restoration, Beaufort-Mackenzie Basin and Mackenzie Corridor, Northern Canada (1). AAPG Bull. 76(8), 1170–1189.

Jakobsson, M., Macnab, R., Mayer, L., Anderson, R., Edwards, M., Hatzky, J., Schenke, H.W., Johnson, P., 2008. An improved bathymetric portrayal of the Arctic Ocean: implications for ocean modelling and geological, geophysical and oceanographic analyses. Geophys. Res. Lett. 35.

Japsen, P., 1993. Influence of lithology and Neogene uplift on seismic velocities in Denmark – Implications for depth conversion of maps. AAPG Bull. 77, 194–211.

Japsen, P., 1998. Regional velocity-depth anomalies, North Sea Chalk: a record of overpressure and Neogene uplift and erosion. AAPG Bull. 82, 2031–2074.

Japsen, P., 1999. Overpressured Cenozoic shale mapped from velocity anomalies relative to a baseline for marine shale, North Sea. Pet. Geosci. 5, 321–336.

Japsen, P., 2000. Investigation of multi-phase erosion using reconstructed shale trends based on sonic data. Sole Pit axis, North Sea. Glob. Planet. Change 24, 189–210.

Japsen, P., Green, P.F., Chalmers, J.A., 2005. Separation of Palaeogene and Neogene uplift on Nuussuaq, West Greenland. J. Geol. Soc. London 162, 299–314.

Japsen, P., Mukerji, T., Mavko, G., 2007. Constraints on velocity□depth trends from rock physics models. Geophys. Prospect. 55, 135–154.

Karlsen, D.A., Skeie, J.E., Backer-Owe, K., Bjørlykke, K., Olstad, R., Berge, K., Cecchi, M., Schaefer, R.G., 2004. Petroleum migration, faults and overpressure. Part II. Case history: The Haltenbanken Petroleum Province, offshore Norway, In: J.M. Cubbit, W.A. England, S., Larter (Eds.), Understanding petroleum reservoirs: Towards an integrated reservoir

engineering and geochemical approach: Geological Society, London, Special Publications, 237, pp. 305–372.

Laberg, J.S., Andreassen, K., Vorren, T.O., 2012. Late Cenozoic erosion of the high-latitude southwestern Barents Sea shelf revisited. Bull. Geol. Soc. Am. 124, 77–88.

Lerche, I., 1997. Erosion and uplift uncertainties in the Barents Sea, Norway. Math. Geol. 29, 469–501.

Løseth, H., Lippard, S.J., Sættem, J., Fanavoll, S., Fjerdingstad, V., Leith, T.L., Ritter, U., Smelror, M., Sylta, Ø., 1993. Cenozoic uplift and erosion of the Barents Sea-evidence from the Svalis Dome area. Arctic Geol. Petrol. Potential Nor. Petrol. Soc. Spec. Publ. 2, 643–664.

Lothe, A.E., Borge, H., Gabrielsen, R.H., 2004. Modelling of hydraulic leakage by pressure and stress simulations and implications for Biot's constant: an example from the Halten Terrace, offshore Mid-Norway. Petrol. Geoscience 10 (3), 199–213.

Magara, K., 1976. Thickness of removed sedimentary rocks, paleopore pressure, and paleotemperature, southwestern part of Western Canada Basin. AAPG Bull. 60, 554.

Mondol, N.H., 2009. Porosity and Permeability Development in Mechanically Compacted Silt-kaolinite Mixtures. SEG Technical Program Expanded Abstracts, pp. 2139–2143.

Mørk, M.B.E., Duncan, R.A., 1993. Late Pliocene basaltic volcanism on the Western Barents Shelf margin: implications from petrology and 40Ar–39Ar dating of volcanoclastic debris from a shallow drill core. Nor. Geol. Tidsskr. 73, I993.

Nansen, F., 1904. The Bathymetrical Features of the North Polar Seas with a Discussion of the Continental Shelves and Previous Oscillations of the Shoreline: Norwegian Polar Expeditions 1893-1896, Scientific Results Volume 4: Christiania, Jacob Dybwad, 231 p.

Nasuti, A., Roberts, D., Gernigon, L., 2015. Multiphase mafic dykes in the Caledonides of northern Finnmark revealed by a new high resolution aeromagnetic dataset. Norwegian J. Geol. 95, 285–297.

Norwegian Interactive Offshore Stratigraphic Lexicon. NORLEX. http://www.nhm2.uio.no/norlex/ (accessed June, 2014).

Norwegian Petroleum Directorate (NPD), 2014. Barents Sea Structural Elements Map. http://gis.npd.no/factmaps/html_20/ (accessed June, 2014).

Norwegian Petroleum Directorate (NPD), 2014. NPD FactPages http://factpages.npd.no/factpages/Default.aspx?culture=en (accessed April, 2015).

Nyland, B., Jensen, L.N., Skagen, J., Skarpnes, O., Vorren, T., 1992. Tertiary uplift and erosion in the Barents Sea: magnitude, timing and consequences. In: Larsen, R.M., Brekke, H., Larsen, B.T., Talleraas, E. (Eds). Structural and Tectonic Modelling and its Application to Petroleum Geology. Norwegian Petroleum Society, NPF Special Publication, 1, Elsevier, Amsterdam, pp. 153–162.

Ohm, S.E., Karlsen, D.A., Austin, T.J.F., 2008. Geochemically driven exploration models in uplifted areas: example from the Norwegian Barents Sea. AAPG Bull. 92, 1191–1223.

Peikert, E.W., 1985. Stratigraphic velocity interpretation: National Petroleum Reserve—Alaska. Seismic stratigraphy II: An integrated approach to hydrocarbon exploration: AAPG Memoir 39, 7–36.

Rasmussen, E., Fjeldskaar, W., 1996. Quantification of the Pliocene-Pleistocene erosion of the Barents Sea from present-day bathymetry. Glob. Planet. Change 12, 119–133.

Reemst, P., Cloetingh, S., Fanavoll, S., 1994. Tectonostratigraphic modelling of Cenozoic uplift and erosion in the south-western Barents Sea. Mar. Petrol. Geol. 478–490.

Richardsen, G., Henriksen, E., Vorren, T.O., 1991. Evolution of the Cenozoic sedimentary wedge during rifting and seafloor spreading west of the Stappen High, western Barents Sea. Mar. Geol. 101 (1–4), 11–30.

Richardsen, G., Vorren, T.O., Torudbakken, B.O., 1993. Post-Early Cretaceous uplift and erosion in the southern Barents Sea: a discussion based on analysis of seismic interval velocities. Nor. Geol. Tidsskr. 73, 3–20.

Riis, F., 1996. Quantification of Cenozoic vertical movements of Scandinavia by correlation of morphological surfaces with offshore data. Glob. Planet. Change 12(1), 331–357.

Riis, F., Fjeldskaar, W., 1992. On the magnitude of the late Tertiary and Quaternary erosion and its significance for the uplift of Scandinavia and the Barents Sea. In: Larsen, R.M., Brekke,

Ritzmann, O., Faleide, J.I., 2009. The crust and mantle lithosphere in the Barents Sea-Kara Sea region. Tectonophysics 470, 89–104.

Ryseth, A., Augustson, J.H., Charnock, M., Haugerud, O., Knutsen, S.M., Midbøe, P.S., Opsal, J.G., Sundsbø, G., 2003. Cenozoic stratigraphy and evolution of the Sørvestsnaget Basin, southwestern Barents Sea. Nor. Geol. Tidsskr. 83, 107–130.

Rønnevik, H., Jacobsen, H.P., 1984. Structural highs and basins in the western Barents Sea. In: A.M. Spencer et al. (Eds.): Petroleum Geology of the North European margin. Norwegian Petroleum Society (Graham & Trotman), 98–107.

Sclater, J.G., Christie, P.A.F., 1980. Continental stretching; an explanation of the post-Mid-Cretaceous subsidence of the central North Sea basin. J. Geophys. Res. 85 (B7), 3711–3739.

Scherbaum, F., 1982. Seismic Velocities in Sedimentary–Rocks–Indicators of Subsidence and Uplift. Geol. Rundsch. 71, 519–536.

Sejrup, H.P., Larsen, E., Haflidason, H., Berstad, I.M., Hjelstuen, B.O., Jonsdottir, H.E., King, E.L., Landvik, J., Longva, O., Nygård, A., Ottesen, D., Raunholm, S., Rise, L., Stalsberg, K., 2003. Configuration, history and impact of the Norwegian Channel Ice Stream. Boreas, 32(1), 18–36.

Schmoker, J.W., Halley, R.B., 1982. Carbonate Porosity versus Depth: A predictable Relation for South Florida: AAPG Bull. 66 (12), 2561–2570.

Smelror, M., Petrov, O.V., Larssen, G.B., Werner, S.C., 2009. Geological history of the Barents Sea. Norges Geol. undersøkelse, 1–135.

Smith, T.M., Sondergeld, C.H., 2001. Examination of AVO responses in the eastern deepwater Gulf of Mexico. Geophysics 66, 1864–1876.

Storvoll, V., Bjørlykke, K., Mondol, N.H., 2005. Velocity-depth trends in Mesozoic and Cenozoic sediments from the Norwegian shelf. AAPG Bull. 89, 359–381.

Tassone, D.R., Holford, S.P., Duddy, I.R., Green, P.F., Hillis, R.R., 2014. Quantifying Cretaceous–Cenozoic exhumation in the Otway Basin, southeastern Australia, using sonic transit time data: implications for conventional and unconventional hydrocarbon prospectivity. AAPG Bull. 98, 67–117.

Thomson, K., Green, P.F., Whitham, A.G., Price, S.P., Underhill, J.R., 1999. New constraints on the thermal history of North-East Greenland from apatite fission-track analysis. Geol. Soc. Am. Bull. 111, 1054–1068.

Tsikalas, F., Faleide, J.I., Eldholm, O., Blaich, O.A., 2012. The NE Atlantic conjugate margins. In: Roberts, D. G., & Bally, A. W. (Eds.), (2012). Regional geology and tectonics: Phanerozoic passive margins, cratonic basins and global tectonic maps, Elsevier, pp. 140–201.

Van Balen, R.T., Skar, T., 2000. The influence of faults and intraplate stresses on the overpressure evolution of the Halten Terrace, mid-Norwegian margin. Tectonophysics, 320 (3), 331–345.

Vassmyr, S., 1989. Barents Sea Conference workshop. Harstad. Abstract.

Vorren, T.O., Richardsen, G., Knutsen, S.M., Henriksen, E., 1991. Cenozoic erosion and sedimentation in the western Barents Sea. Mar. Petrol. Geol. 8, 317–340.

Wells, P.E., 1990. Porosities and seismic velocities of mudstones from Wairarapa and oil-wells of North Island, New-Zealand, and their use in determining burial history. New Zeal. J. Geol. Geop. 33, 29–39.

Worsley, D., 2008. The post□Caledonian development of Svalbard and the western Barents Sea. Polar Res. 27, 298–317.

Wyllie, M.R.J., Gregory, A.R., Gardner, L.W., 1956. Elastic wave velocities in heterogeneous and porous media. Geophysics 21, 41–70.

Wyllie, M.R.J., Gregory, A.R., Gardner, G.H.F., 1958. An experimental investigation of factors affecting elastic wave velocities in porous media. Geophysics 23, 459–493.

Zattin, M., Andreucci, B., de Toffoli, B., Grigo, D., Tsikalas, F., 2016. Thermochronological constraints to late Cenozoic exhumation of the Barents Sea Shelf. Mar. Petrol. Geol. 73, 97–104.

Figure and Table Captions

Figure 1. Map of the southwestern Barents Sea showing the different structural elements and oil-gas discoveries. The regional profiles A-A', and B-B' and the wells studied along the lines are indicated with a red colour and red dots, respectively. The location of the study area is indicated in the inserted figure. Modified from the Norwegian Petroleum Directorate (NPD, 2014, http://gis.npd.no/factmaps/html_20/) and Jakobsson et al. (2008).

Figure 2. North-south geoseismic profile B-B' across the Finnmark Platform. This cross section shows thick Mesozoic strata below extensively truncated layers from the uplifted shelf to the south, left hand side of the profile. The box on the right corner shows the approximate age of the various units. For the location of the 2D line see Fig. 1.

Figure 3. Regional geoseismic profile A-A' running from the southeast to the southwest. This cross-section illustrates the basin configuration, the changes in structural styles and geometries. Areas with missing sections and major erosion can be identified along the profile. For the location of the 2D line see Fig. 1.

Figure 4. Tectonostratigraphic chart from the southwestern Barents Sea, showing the general stratigraphy and the major tectonic events. Modified from Ohm et al. (2008) and Norwegian Interactive Offshore Stratigraphic Lexicon (NORLEX, http://www.nhm2.uio.no/norlex/).

Figure 5. (a) Location map showing the studied wells (40) from the Norwegian Continental Shelf (NCS). (b) The location of the reference wells with no erosion in the Norwegian Sea

and North Sea areas used in this study, are marked by red dots along with the well name according to the Norwegian Petroleum Directorate (NPD FactPages, http://factpages.npd.no/factpages/).

Figure 6. Bathymetric map of the southwestern Barents Sea, showing the location of the wells used in the study area.

Figure 7. Different Normal Compaction Trend (NCT) models for shale and for in-situ sands containing different fluids from First Geo (modified from Gardner et al., 1974) and Japsen et al., 2000; 2007).

Figure 8. Example from the North Sea well 31/4-3 and Norwegian Sea well 6305/1-1 applying different Normal Compaction Trend models for shale, sandstone and limestone. (a) The NCT model of First Geo (modified from Gardner et al., 1974) and (b) the NCT model of Japsen et al. (2000; 2007). Both wells are undercompacted (overpressure) and have the same pattern with different lithology. Geological factors that affect the sonic velocity are shown with black arrows. sst: sandstone, clst: claystone. For the location of the studied wells see Fig. 5. As shown, it is a challenge to make one single NCT model which works for both of these wells.

Figure 9. Schematic overview of the workflow for establishing the Normal Compaction Trend model and a net erosion map based on well log data.

Figure 10. The new calibrated "Dikte NCT model" constructed in this study for the Cretaceous shale (CretShale) and Lower Jurassic-Triassic (LJurTrias) units, which are mixed

sand-shale lithologies deposited in a coastal plain to shallow marine environment. The Y axis corresponds to the depth below the ground surface (or seabed) and the X axis represent the corresponding velocity for the baselines.

Figure 11. Conceptual figure of the Dikte NCT model illustrates how the net apparent erosion is unravelled by matching by best fit the sonic log against the shale and sandstone curves. (a) Initially, the NCTs for shale and sandstone do not fit with the log. (b) Matching of the wells against the zero net erosion baselines requires a shift of the log curve downwards representing the amount of net apparent erosion; i.e. the amount of erosion is determined from the distance between the seabed at present day and the base level of the maximum burial axis.

Figure 12. The established NCT model for shale and sandstone calibrated to reference wells with no net erosion in the North Sea and Norwegian Sea (for the well tops abbreviations see Table 1 and for the location of the wells see Fig. 5b). In wells with no net erosion, the present water depth is shown.

Figure 13. Sonic velocity measurements vs. maximum depth of burial from the studied wells in the southwestern Barents Sea. The estimation of net erosion observed in the wells is based on the NCT model established in this study. For the well top abbreviations see Table 1 and for the location of the wells Fig. 6.

Figure 14. Sonic velocity measurements vs. maximum depth of burial from the exploration wells 7128/6-1 and 7128/4-1 in the Finnmark Platform, southern Barents Sea.

Figure 15. Regional map illustrating the estimated net erosion for the southwestern Barents

Sea, based on sonic log data. In areas that there is no well control, seismic data have been studied to complete the map (see also Table 3).

Figure 16. Previous uplift and net erosion maps for the Barents Sea indicating a general trend of uplift and net erosion increasing towards the East and North. In some areas rather large differences in the estimates can be observed.

Table 1. Abbreviation of the well tops from NPD used for the velocity vs. depth plots of wells on the Norwegian Continental Shelf.

Table 2. Normal Compaction Trend (baselines) for the Cretaceous shale and Lower Jurassic-Triassic units in the southwestern Barents Sea.

Table 3. Apparent net erosion estimates for the studied southwestern Barents Sea wells. For the location of the wells see Fig. 6.

Well Tops	Abbreviation
Water depth + Kelly bushing	Seabed
Paleogene (Sotbakken/Hordaland Group)	Paleogene
Top Cretaceous (Nygrunnen/Shetland Group)	TC
Adventdalen/Cromer Knoll Group	Cromer
Base Cretaceous (Viking Group/Hekkingen formation)	BC
Base Jurassic (Kapp Toscana Group/"Gray Beds")	BJ
Intra Base Triassic (Sassendalen Group)	InBTr
Base Triassic (Sassendalen Group)	BTr
Base Permian (Gipsdalen Group)	BPerm
Base Carboniferous (Billefjorden Group)	BCarb

Table 1

Cretaceous Shale		L.Jurassic-Triassic	
Velocity (Vsh, m/s)	Depth (m)	Velocity (Vsh, m/s)	Depth (m)
1098.154	0	1543.154	0
1099.289	1.313	1549.06	6.833
1099.289	1.313	1549.06	6.833
1103.679	6.392	1551.799	10.002
1103.679	6.392	1551.799	10.002
1106.158	9.261	1556.995	15.545
1106.158	9.261	1556.995	15.545
1106.799	10.002	1561.175	20.004
1106.799	10.002	1561.175	20.004
1108.015	11.299	1570.023	29.443
1108.015	11.299	1570.023	29.443
1116.175	20.004	1570.551	30.006
1116.175	20.004	1570.551	30.006
1121.043	25.197	1571.906	31.452
1121.043	25.197	1571.906	31.452
1125.551	30.006	1579.927	40.008
1125.551	30.006	1579.927	40.008
1134.071	39.095	1583.051	43.341
1134.071	39.095	1583.051	43.341
1134.927	40.008	1589.302	50.01
1134.927	40.008	1589.302	50.01
1137.124	42.352	1596.079	57.239
1137.124	42.352	1596.079	57.239
1144.302	50.01	1598.678	60.012
1144.302	50.01	1598.678	60.012
1147.099	52.993	1605.351	67.142
1147.099	52.993	1605.351	67.142
1153.678	60.012	1608.039	70.014
1153.678	60.012	1608.039	70.014
1160.112	66.887	1609.06	71.123
1160.112	66.887	1609.06	71.123
1163.039	70.014	1617.246	80.016
1163.039	70.014	1617.246	80.016
1170.569	78.194	1621.764	84.924

Table 2

The remaining part of this large table is enclosed as

"Appendix A. Supplementary data".

X coordinates	Y coordinates	Net erosion (m)	Uncertainty (±m)	Well name
429692	7869590	1800	300	7019/1-1
390813	7922856	1000	50	7117/9-1
437872	7922575	1750	100	7119-7-1
475817	7980020	1750	100	7120/1-1 R2
491170	7890289	1600	50	7120/12-1
492969	7891571	1600	50	7120/12-2
481924	7987306	1750	150	7120/2-1
489425	7932810	1700	200	7120/9-2
514307	7944422	1650	100	7121/5-1
523051	7952738	1750	100	7121/5-2
523421	7935227	1700	100	7121/5-3
525525	7906075	1650	100	7121/9-1
556833	7985596	1600	200	7122/2-1
632001	7966518	1400	50	7124/3-1
641392	7943214	1400	100	7125/4-2
749765	7952606	1450	150	7128/4-1
775927	7953278	1500	100	7128/6-1
348693	7996429	361	-	7216/11-1 S
477634	8044086	1750	100	7220/8-1
550640	7997835	1600	200	7222/11-1 T2
612059	8024028	1600	100	7224/7-1
744329	8099458	2250	100	7228/2-1 S
759926	8050128	2000	100	7228/9-1 S
793702	8034371	1700	200	7229/11-1
355518	8164236	800	100	7316/5-1
502403	8148910	2500	200	7321/7-1
513312	8138308	2200	100	7321/8-1
607068	8121933	2100	200	7324/10-1

Table 3

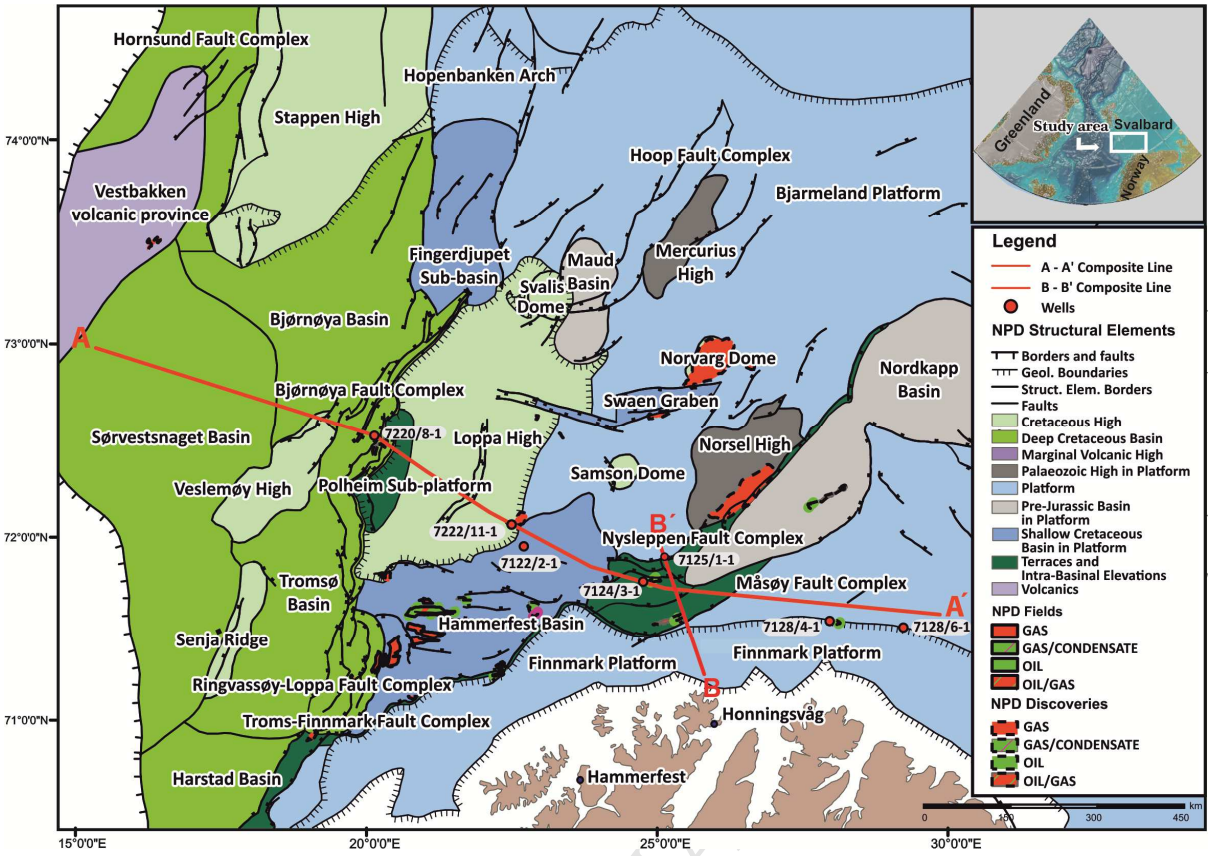

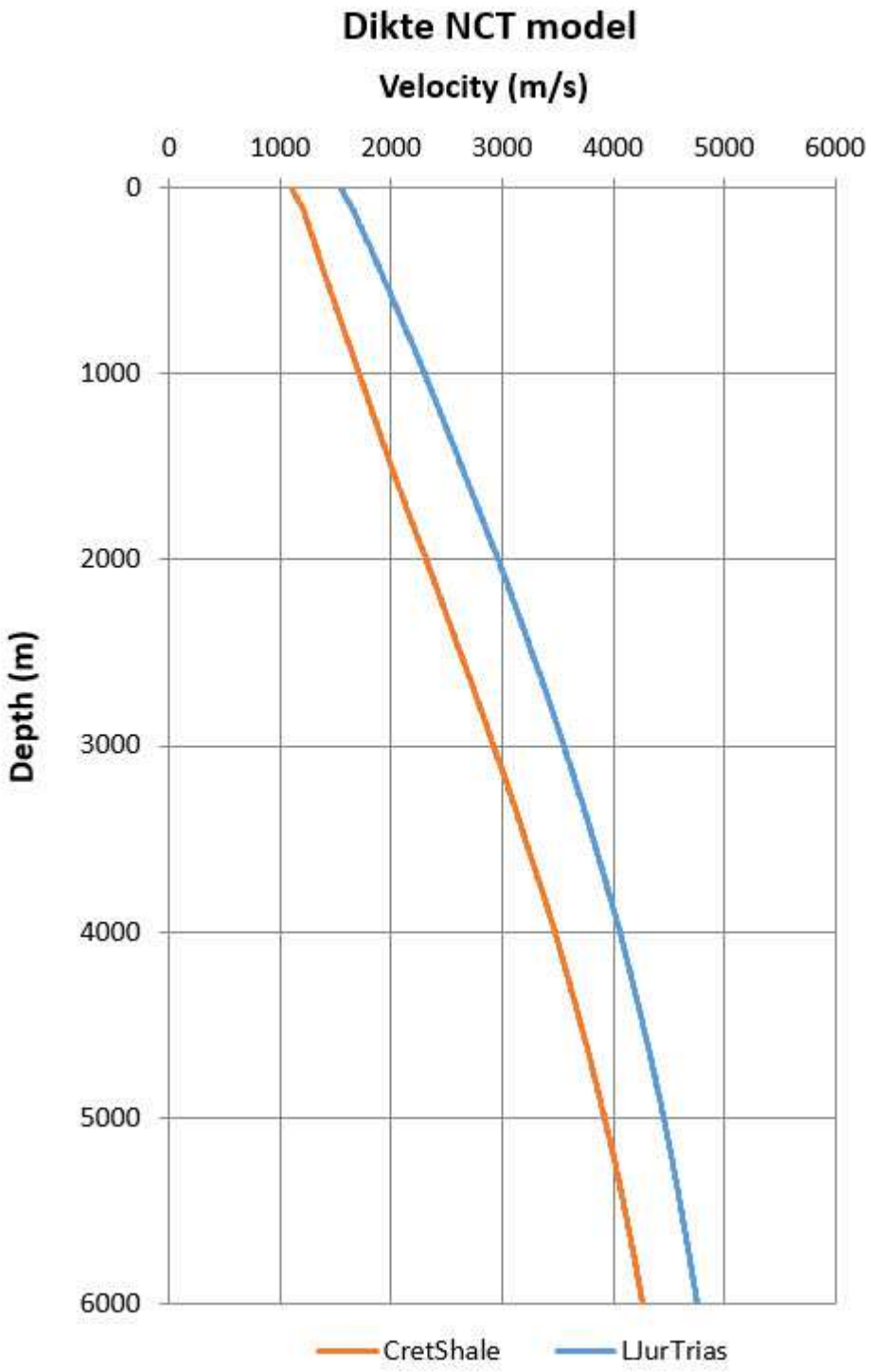
Dikte NCT model
Velocity (m/s)
0
1000
2000
3000
4000
5000
6000
Depth (m)
0
1000
2000
3000
4000
5000
6000
CretShale
LJurTrias

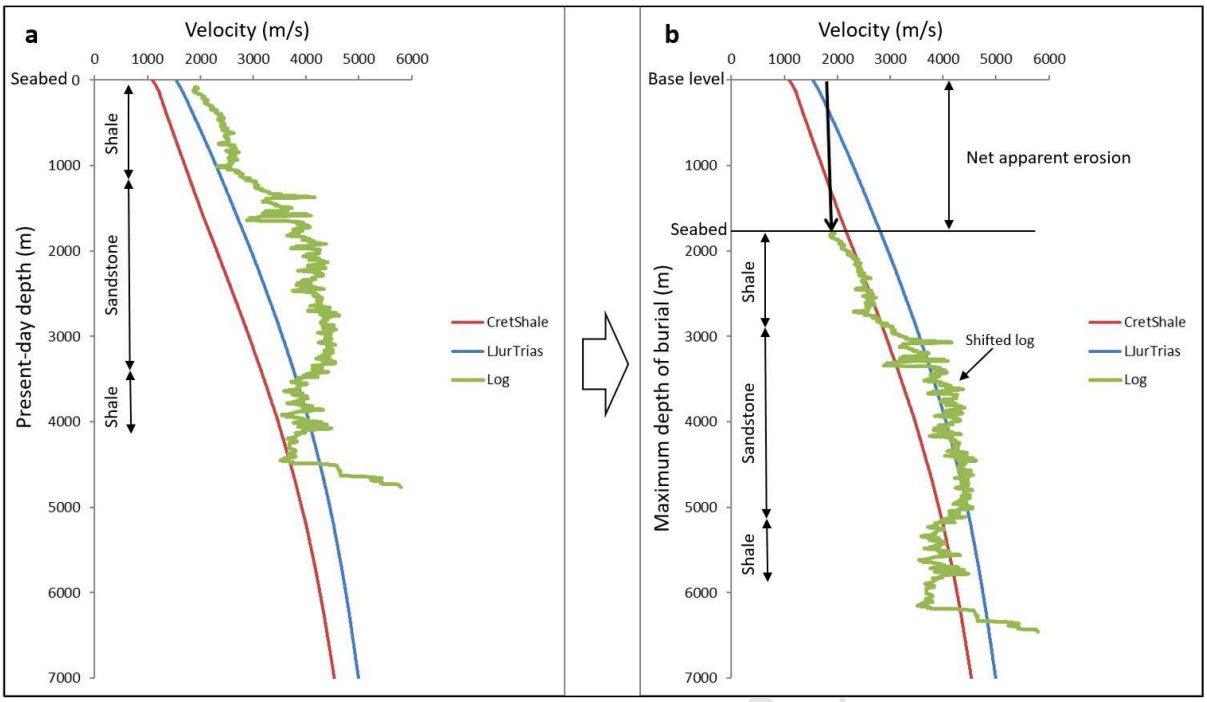

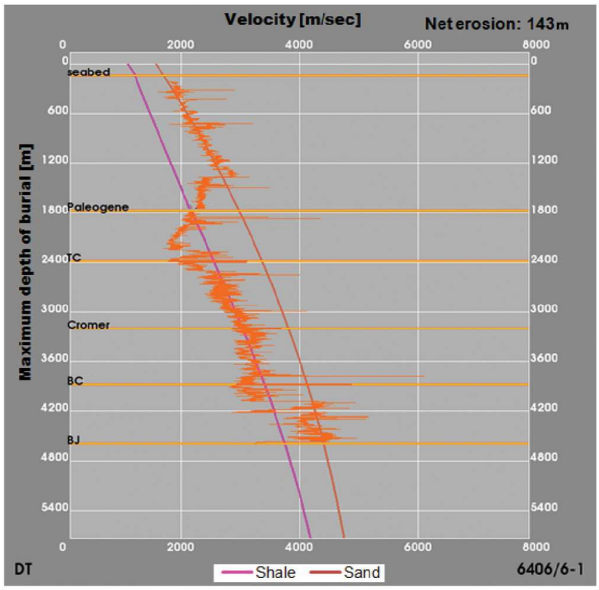
Velocity [m/sec]
Net erosion: 143m
Maximum depth of burial [m]
seabed
Paleogene
TC
Cromer
BC
BJ
DT
Shale
Sand
6406/6-1

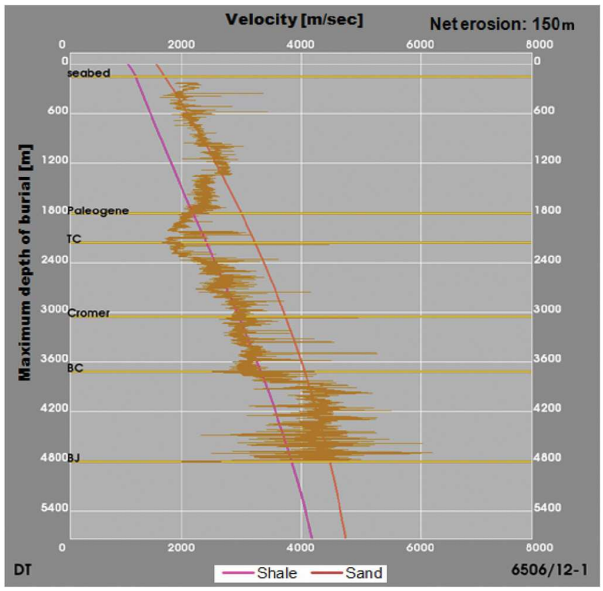
Velocity [m/sec]
Net erosion: 150m
Maximum depth of burial [m]
seabed
Paleogene
TC
Cromer
BC
BJ
DT
Shale
Sand
6506/12-1

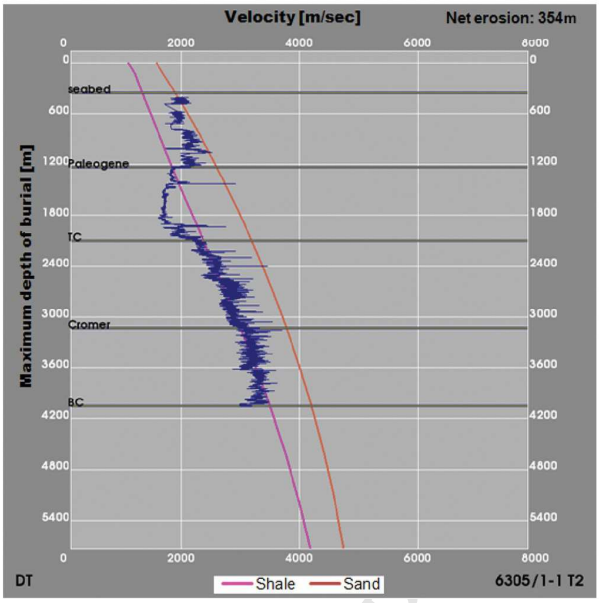
Velocity [m/sec]
Net erosion: 354m
Maximum depth of burial [m]
seabed
Paleogene
TC
Cromer
BC
DT
Shale
Sand
6305/1-1 T2

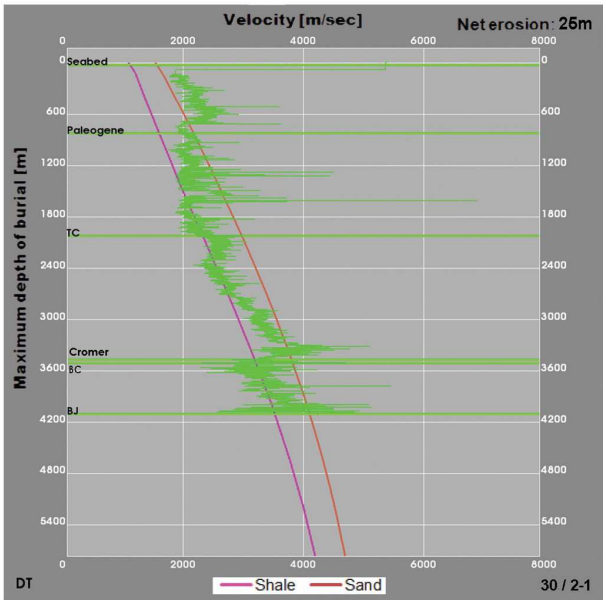
Velocity [m/sec]
Net erosion: 26m
Maximum depth of burial [m]
Seabed
Paleogene
TC
Cromer
BC
BJ
DT
Shale
Sand
30 / 2-1

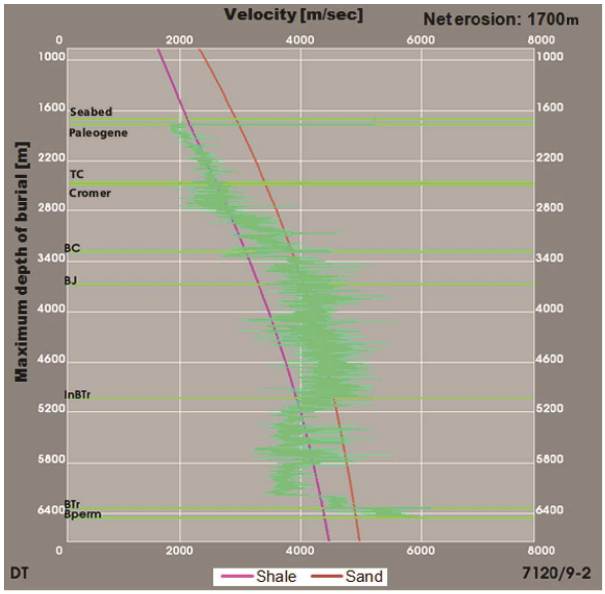
Velocity [m/sec]
Net erosion: 1700m
Maximum depth of burial [m]
Seabed
Paleogene
TC
Cromer
BC
BJ
InBTr
BTr
Bperm
DT
Shale
Sand
7120/9-2

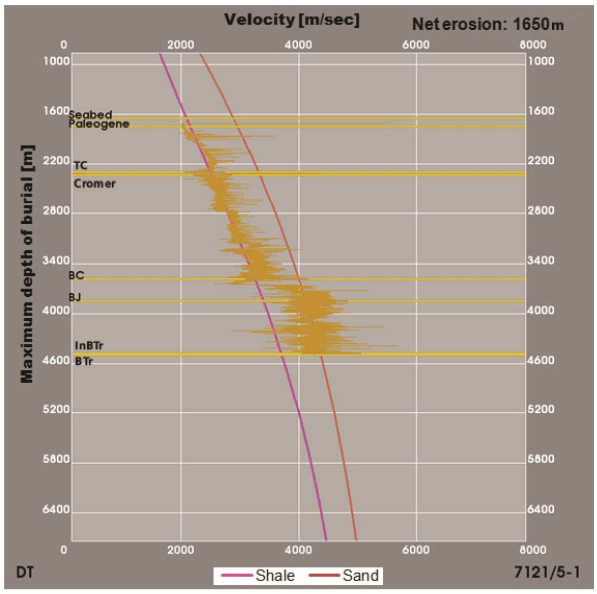
Velocity [m/sec]
Net erosion: 1650m
Maximum depth of burial [m]
Seabed
Paleogene
TC
Cromer
BC
BJ
InBTr
BTr
DT
Shale
Sand
7121/5-1

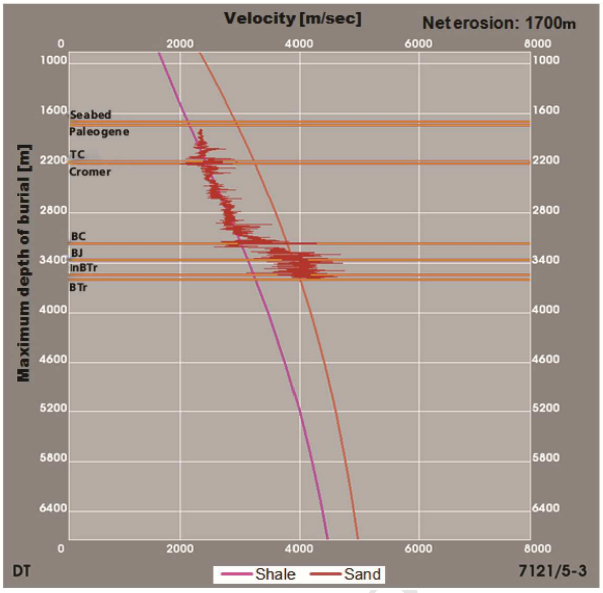
Velocity [m/sec]
Net erosion: 1700m
Maximum depth of burial [m]
Seabed
Paleogene
TC
Cromer
BC
BJ
InBTr
BTr
DT
Shale
Sand
7121/5-3

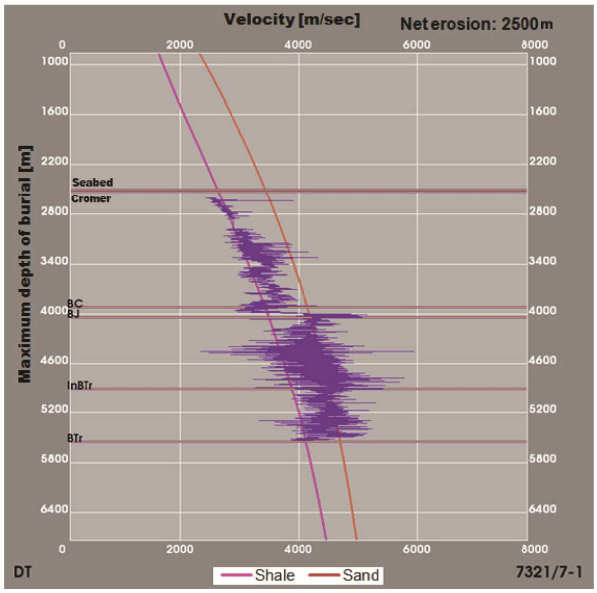
Velocity [m/sec]
Net erosion: 2500m
Maximum depth of burial [m]
Seabed
Cromer
BC
BJ
InBTr
BTr
DT
Shale
Sand
7321/7-1

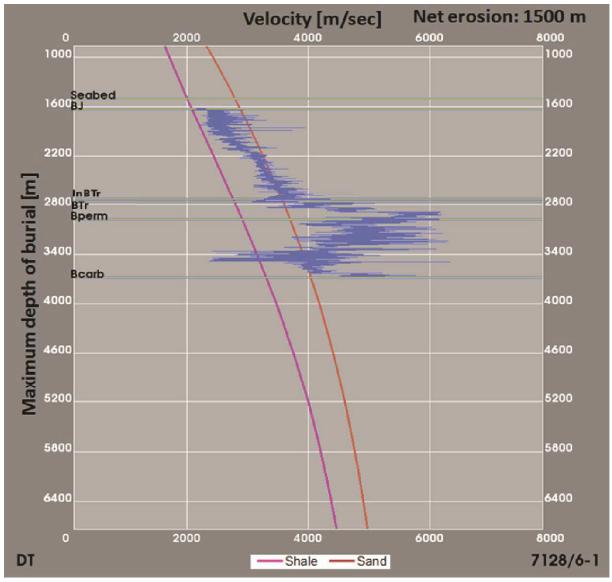

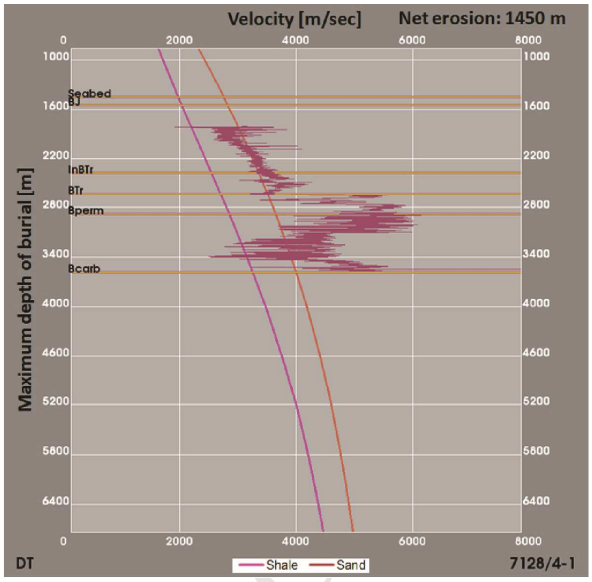

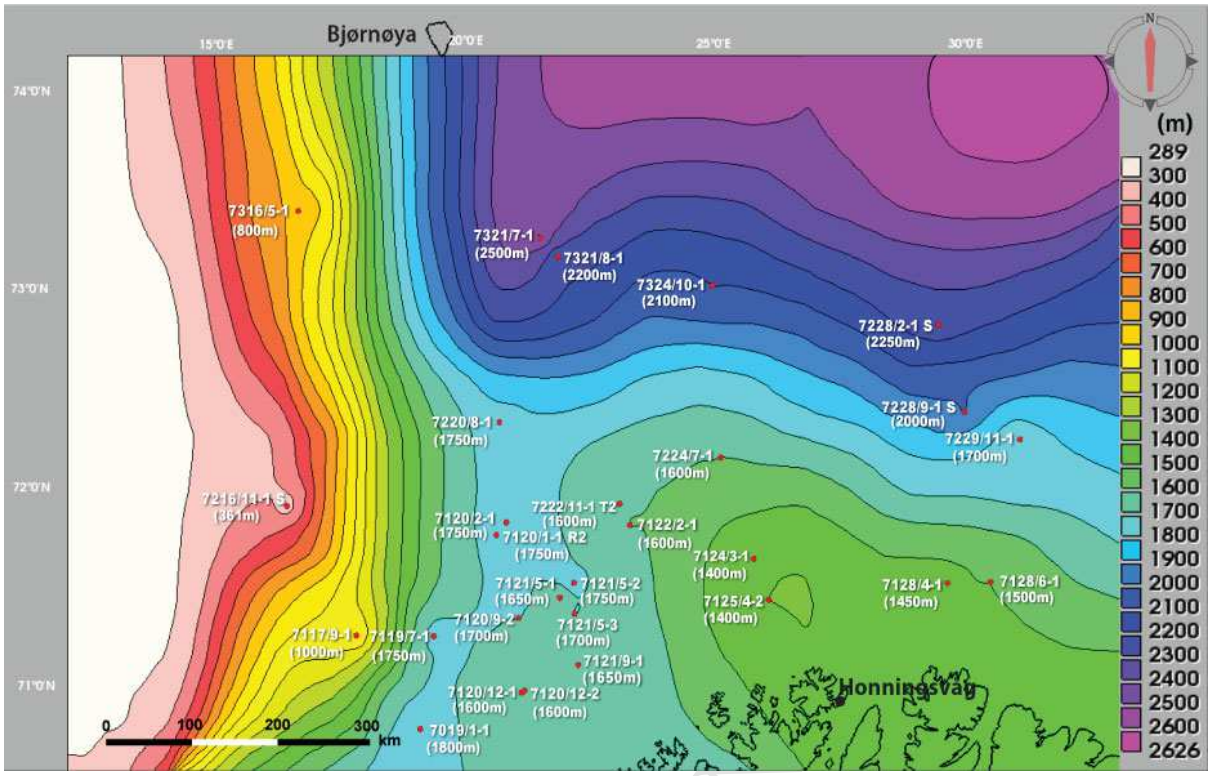

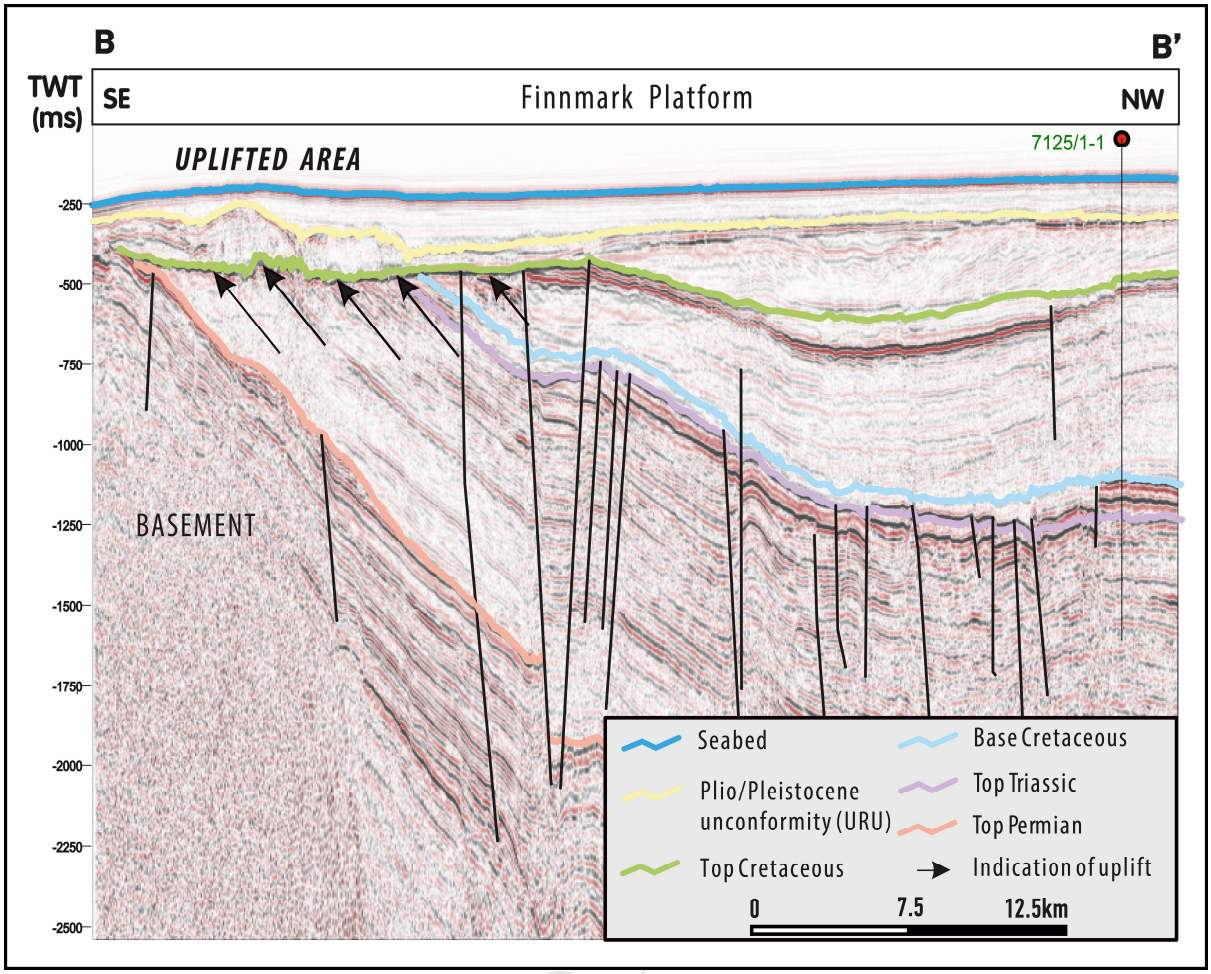
B
B'
TWT (ms)
SE
Finnmark Platform
NW
UPLIFTED AREA
7125/1-1
-250
-500
-750
-1000
-1250
-1500
-1750
-2000
-2250
-2500
BASEMENT
Seabed
Plio/Pleistocene unconformity (URU)
Top Cretaceous
Base Cretaceous
Top Triassic
Top Permian
Indication of uplift
0
7.5
12.5km

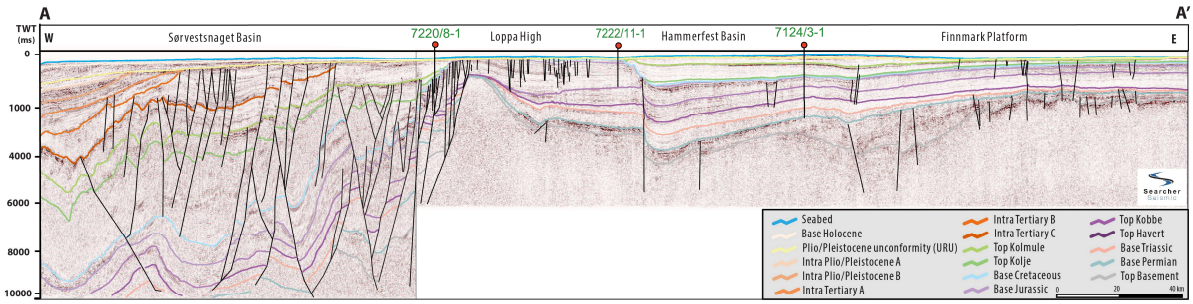

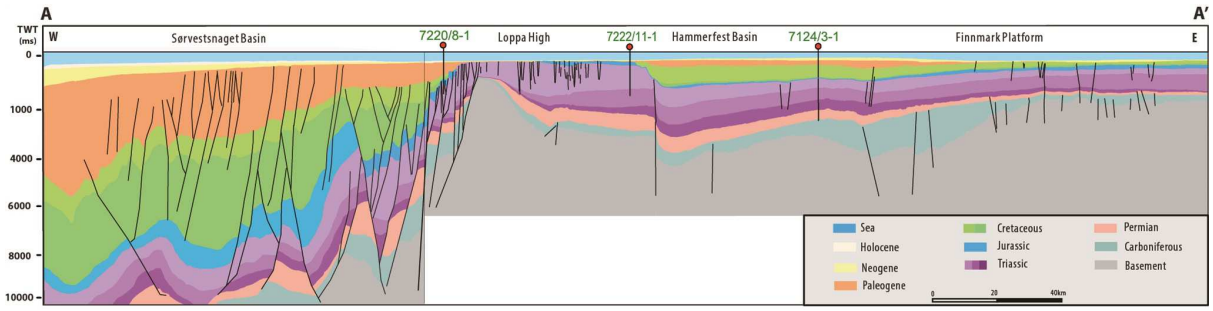

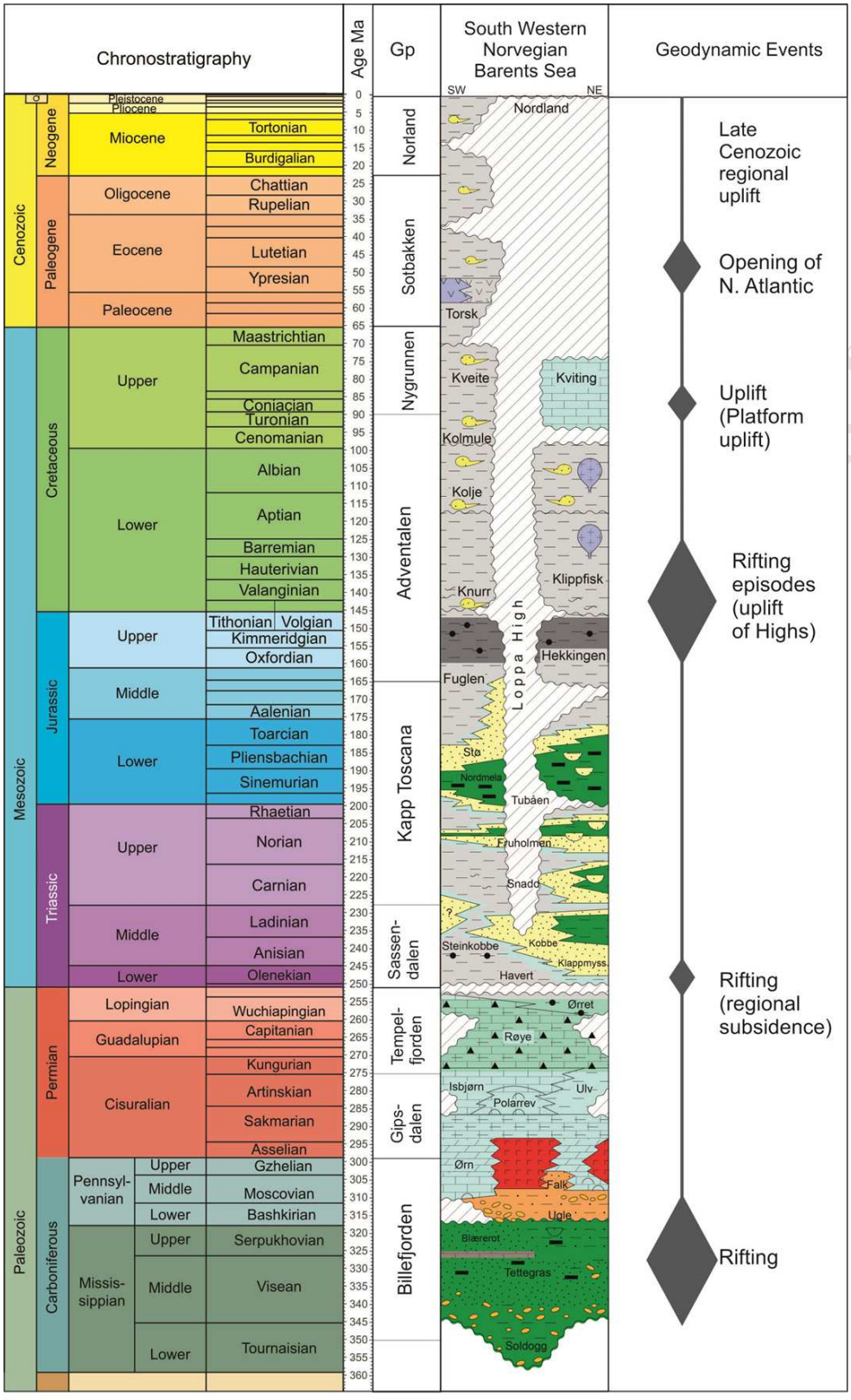
Chronostratigraphy
Age Ma
Gp
South Western Norvegian Barents Sea
SW
NE
Geodynamic Events
Cenozoic
Neogene
Paleogene
Mesozoic
Cretaceous
Jurassic
Triassic
Paleozoic
Permian
Carboniferous
Pleistocene
Pliocene
Miocene
Oligocene
Eocene
Paleocene
Upper
Lower
Middle
Pennsyl-vanian
Missis-sippian
Tortonian
Burdigalian
Chattian
Rupelian
Lutetian
Ypresian
Maastrichtian
Campanian
Coniacian
Turonian
Cenomanian
Albian
Aptian
Barremian
Hauterivian
Valanginian
Tithonian
Volgian
Kimmeridgian
Oxfordian
Aalenian
Toarcian
Pliensbachian
Sinemurian
Rhaetian
Norian
Carnian
Ladinian
Anisian
Olenekian
Lopingian
Guadalupian
Cisuralian
Wuchiapingian
Capitanian
Kungurian
Artinskian
Sakmarian
Asselian
Gzhelian
Moscovian
Bashkirian
Serpukhovian
Visean
Tournaisian
Norland
Sotbakken
Nygrunnen
Adventalen
Kapp Toscana
Sassen-dalen
Tempel-fjorden
Gips-dalen
Billefjorden
Nordland
Torsk
Kveite
Kviting
Kolmule
Kolje
Knurr
Klippfisk
Hekkingen
Loppa High
Fuglen
Stø
Nordmela
Tubåen
Fruholmen
Snadd
Steinkobbe
Kobbe
Klappmyss
Havert
Ørret
Røye
Isbjørn
Ulv
Polarrev
Ørn
Falk
Ugle
Blåerot
Tettegras
Soldogg
Late Cenozoic regional uplift
Opening of N. Atlantic
Uplift (Platform uplift)
Rifting episodes (uplift of Highs)
Rifting (regional subsidence)
Rifting
Legend
Humid terrestrial shales
Arid terrestrial shales
Lacustrine
Shallow marine sst
Deep marine sst
Chalk carbonate
Marine shales and mudstones
Tuff
Conglomerate
Sandstone
Siltstone
Shale
Organic rich
Coal layers
Chert
Marl
Limestone / chalk
Dolomite
Rock salt
Reef build-ups
Base of slope fans
Channel fan systems
Hiatus
Unconformity
Metamorphic basement
Geodynamic events

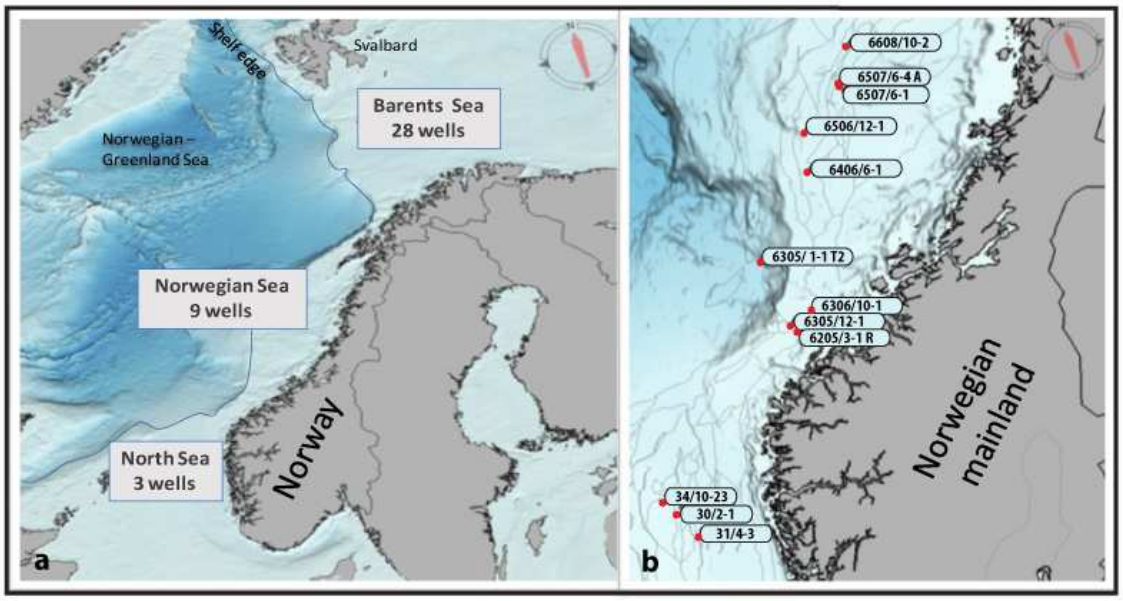

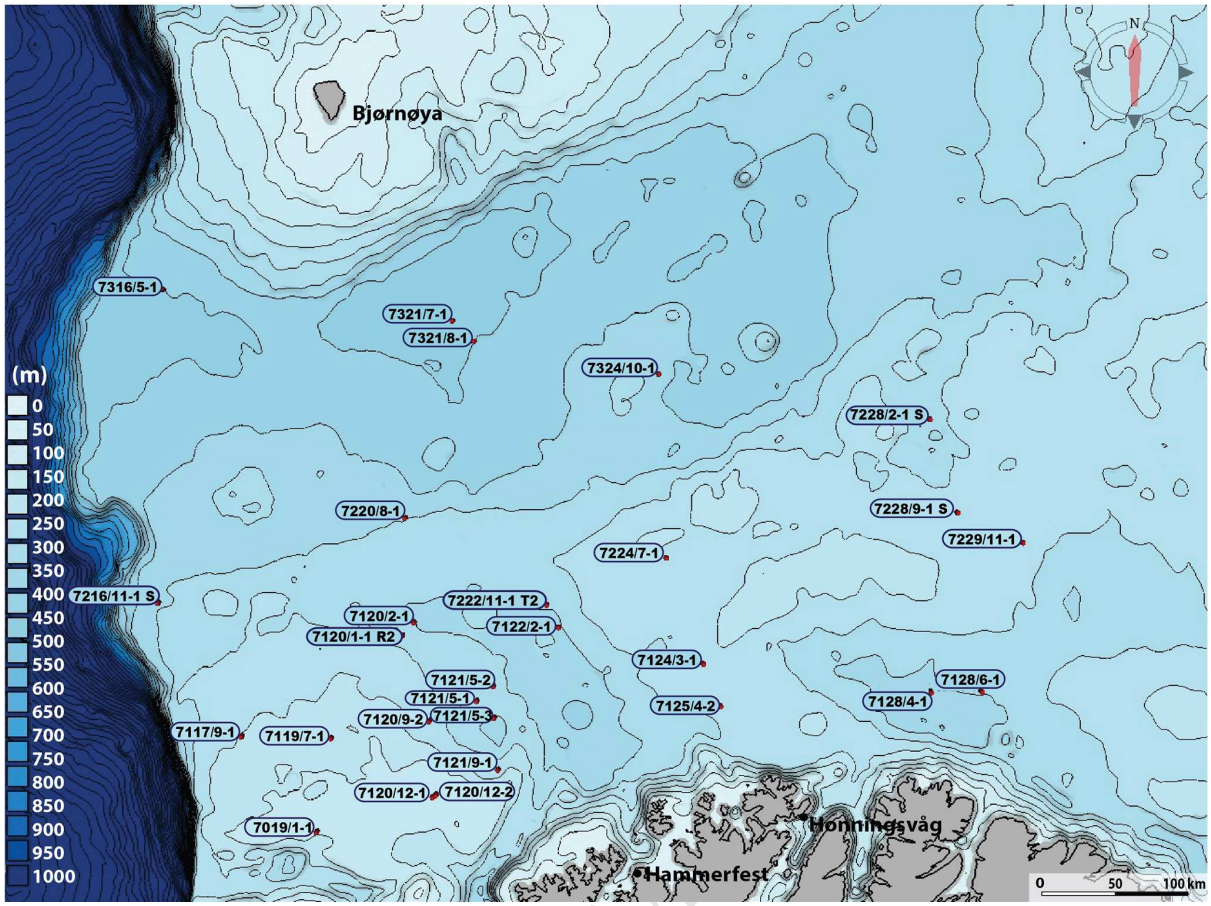

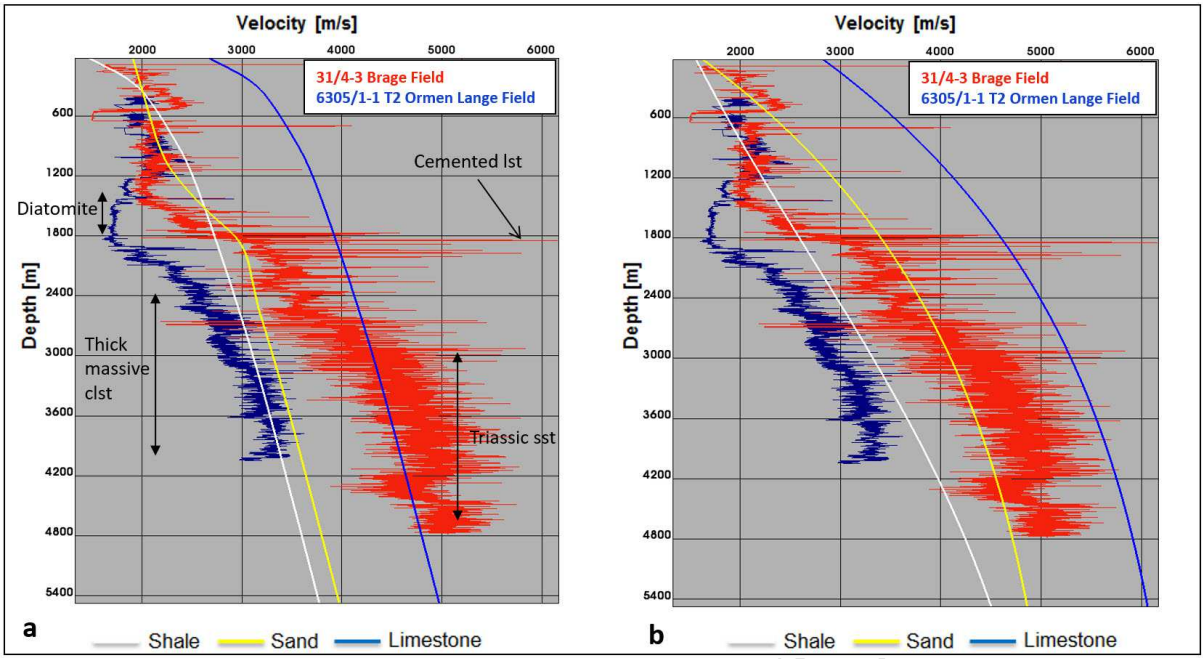

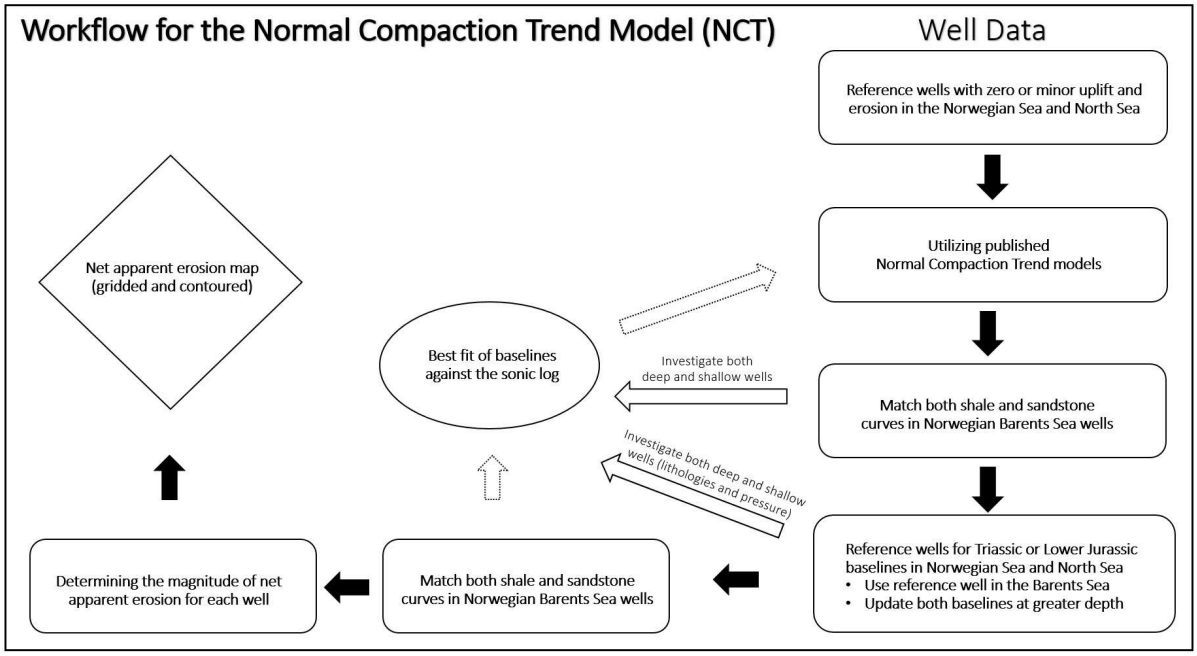

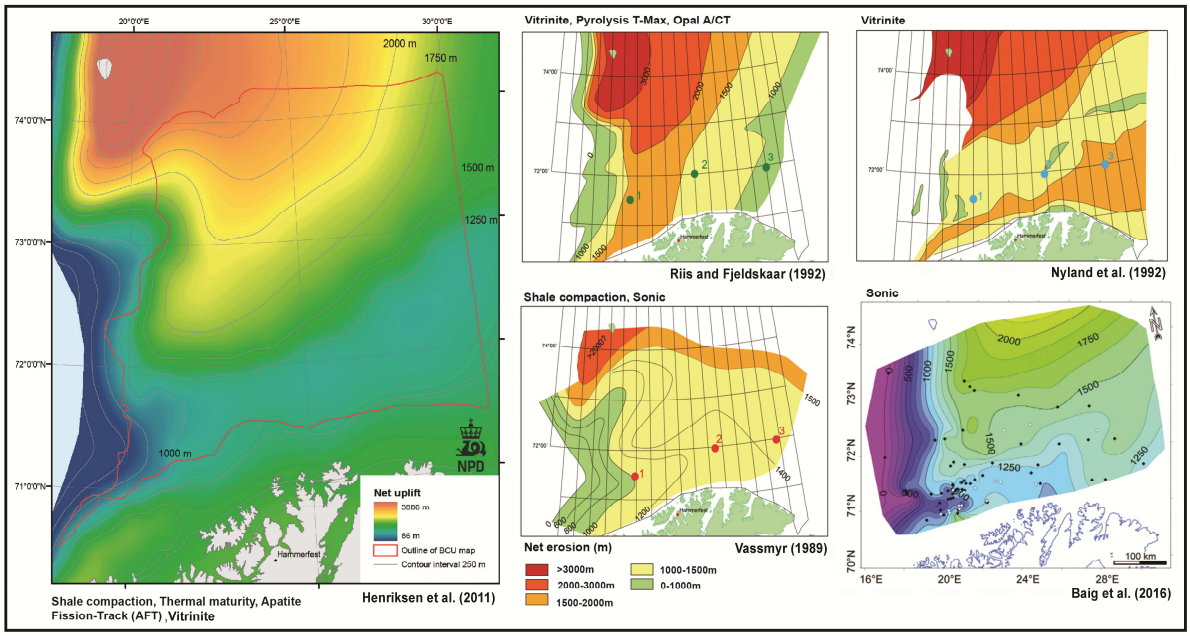

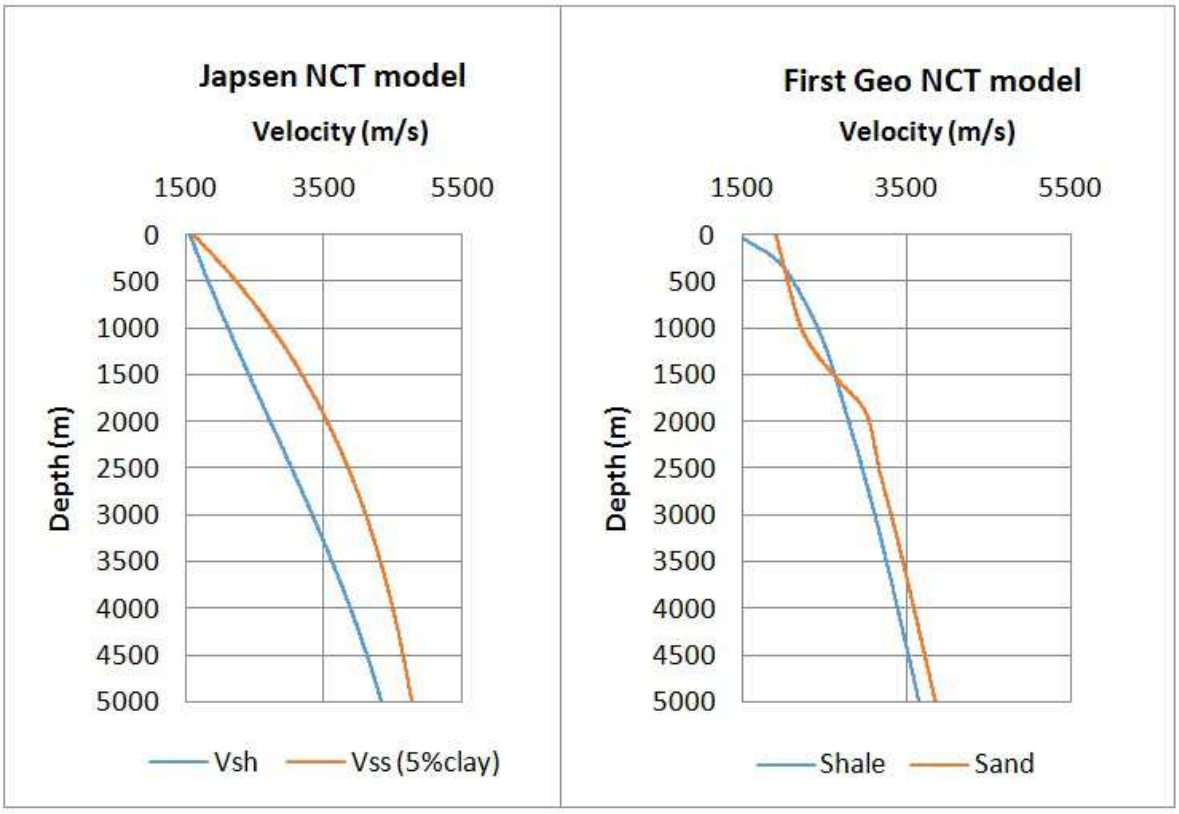

Highlights of the manuscript:

- Net apparent erosion has been estimated for 28 wells in the southwestern Barents Sea, based on well log data and compaction studies. This has resulted in a new contoured map showing the amount and distribution of estimated erosion in the region.

- The net apparent erosion map shows two main regional trends of erosional pattern; an increasing amount of erosion towards the north and a sharp decrease of erosion westwards of the hinge zone into the western Barents Sea. The highest erosion estimates are observed towards Svalbard, with values up to 2500 m.

- A new Normal Compaction Trend (NCT) model for two selected shale and sandstone dominated lithologies is constructed from sonic logs. The shale NCT is calibrated to the Cretaceous shales in the northern part of the North Sea and the Norwegian Sea and applied to the Cretaceous shales of the Barents Sea. The sandstone NCT is calibrated to the Lower Jurassic Åre Formation of the Norwegian Sea and applied to the Lower Jurassic-Upper Triassic coastal plain section of the Barents Sea.

- The new NCT model can address at greater depths (e.g. within the Triassic) compared with other published and unpublished compactions trends.

- The well log based NCT model can be calibrated to other velocity data such as interval velocities in maps and seismic profiles from regional depth conversion. This can be used to estimate net erosion in undrilled areas.